Master in Bioengineering
Specialization in Biological Engineering

Bioremediation of ibuprofen present in water bodies using 3D printed artificial biofilms

Master dissertation

by

Daniel José Rodrigues Trigo

Developed within the scope of the Dissertation course

realized in

Institute of Ecopreneurship, University of Applied Sciences and Arts Northwestern Switzerland

Supervisor in FEUP: **Prof. Olga Nunes**

Supervisor in FHNW: **Prof. Dr. Philippe Corvini**

Supervisor in FHNW: **Dr. Boris Kolvenbach**

Bioengineering department

September 2024

Acknowledgments

In this last step of my master's degree, not only did I had the opportunity to realize this thesis that will allow me to enter in a new chapter of my life but also to do it abroad, where I meet new people, a new culture, and learned about what working means and about myself.

First, I want to thank my professor, Olga Nunes, for presenting this opportunity to go abroad, and who always demonstrated interest in my work.

Then I thank the FNHW, more specifically, Professor Philippe Corvini, for having welcomed and integrated me into his team to develop my thesis. To Doctor Boris Kolvenbach for his guidance and wise advice that put me in a good path.

A special thanks to Ana Ackermann, who did a closer supervision of my work, would always keep in touch to know the last developments of my work and helped shape what I was able to achieve today. Above all, I appreciate her relentless effort to motivate me in my work and writing my thesis.

To all the team, Irena, Marcel, Cri, Fra, Shu Harn, Ramona, Aurelie, Jérôme, Dalila, Bastien to name a few, I appreciate how smoothly and quickly they integrated me, leaving me not time to realize I was living abroad. Also, for letting me be part of their lives, sharing their thoughts about my work and for the happy moments we created.

Living abroad was no easy task, but a lot of people made sure that burden was not for me to carry alone, for that I thank all the people I was able to meet and befriend, Chris, Suzzane, Julien, Alessandro, Esra, Clodoaldo, George, Bert and Virgínia.

But most importantly I'm grateful to my family and friends, who since the beginning incentivized me to seize this opportunity, helped me in the hardest moments and made my time abroad a great experience, that I'll remember for the rest of my life.

To all the people who were part of this stage of my life I'm totally grateful for their contribution.

Abstract

Freshwater is a resource of crucial importance for humanity and a great fraction of human activity relies on it. However, the ever-growing world population results in a corresponding increase in freshwater demand, which is in great part sourced from aquifers, in other words, society relies vastly on groundwater. Conversely, the same human activities that require freshwater often dispose of it in ways that are harmful to the environment. There have been reports of chemicals originating from human activity being detected all around the world, being pharmaceuticals one such group. These compounds, unlike others, are designed to be bioactive and biodegradation resistant when ingested by humans, therefore, these tend to be recalcitrant, resulting in their accumulation in several habitats, and possibly toxic to wildlife, followed by unpredicted outcomes. Therefore, in order to sustain humanity's intrinsic demand for freshwater and, at the same time, preserve the environment and ensure a good public health, measures should be taken to maintain groundwater's quality.

Therefore, this study aimed at developing a bioremediation method that combines the ability of microorganisms to degrade pharmaceuticals with the property of bioprinting to produce a designed 3D-printed artificial biofilm. This approach was assessed by inoculating either bacterial consortia, sourced from wastewater, or strains, isolated form the said consortia, inside an alginate-based hydrogel, followed by its solidification through crosslinking mediated by eosin Y (EY) and triethanolamine (TEA) induced with green light (520 nm). Finally, the ibuprofen concentration was monitored to assess its degradation by the consortia and strains.

Batch experiments were conducted with microorganisms inside a 3D printed gel and the latter in groundwater-like conditions spiked with 10 mg/L of IBU. Two bacterial consortia and one strain were studied, all of which were able to degrade IBU within 100-400 h, while inside a 3D printed gel. The survivability of the consortia in the 3D printed gel was assessed to guarantee its survival for at least two weeks. Moreover, the hydrogel's components demonstrated no toxicity for the consortia, however, it was observed that some components could be used as additional carbon sources diminishing IBU metabolization.

To sum up, a successful 3D printed biofilm was constructed. Its employment into groundwater-like conditions seemed feasible but suffered from some major issues, including the fragmentation of the 3D printed gel and lower degradation rates compared to free cells.

Keywords: groundwater, biofilm, ibuprofen removal, bioprinting, alginate hydrogel.

Declaration

I hereby declare, under vow of honor, that this work is original and that all non-original contributions have been properly referenced with identification of the source.

08/09/2024

Index

1 Introduction 1

2 Context and State of the Art 3

2.1 Threats to groundwater quality 3

2.1.1 Contamination by pharmaceuticals 5

2.2 Ibuprofen 6

2.2.1 Detection of ibuprofen in the environment 7

2.2.2 Impact of ibuprofen in wildlife 7

2.2.3 Current methods to remove ibuprofen from water 10

2.2.4 Biodegradation of ibuprofen 11

2.3 Bioprinting 14

2.3.1 Hydrogel 17

2.3.2 Crosslinking 19

2.4 Aim 21

3 Materials and methods 22

3.1 Media preparation 22

3.1.1 Mineral medium Brunner 22

3.1.2 Ibuprofen stock solution 22

3.1.3 Synthetic sewage 22

3.2 Cells cultivation 22

3.2.1 Incubation 23

3.3 Bioprinting 23

3.3.1 Methacrylic modified sodium alginate preparation 23

3.3.2 Ink preparation 24

3.3.3 3D-bioprinting 24

3.3.4 3D object computer-aided design 24

3.4 Degradation experiment 25

3.4.1 Optical density measurement 25

3.4.2 High performance liquid chromatography 26

3.4.3 Extraction protocol 26
3.4.4 Ink toxicity experiment 26
3.4.5 Survival test 27
3.5 Strain isolation 27
3.5.1 Plate isolation 27
3.5.2 Dilution "isolation" 27
3.6 Statistical analysis 28
4 Results and Discussion 29
4.1 Consortia 29
4.1.1 Degradation experiment 29
4.1.2 Growth curve 31
4.1.3 Survival test 32
4.1.4 Ink toxicity test 33
4.2 Plate isolation 35
4.3 Dilution "isolation" 36
4.4 Isolate 3 39
4.4.1 Degradation experiment 39
4.4.2 Growth curve 40
5 Conclusion 41
5.1 Future work and limitations 41
6 References 43
7 Appendix 50
7.1 Mineral medium Brunner recipe 50
7.2 Gel fragmentation – isolate 3 degradation experiment 51
7.3 Mann-Whitney U test 55
7.3.1 Degradation experiment 55
7.3.2 Survival test 55
7.3.3 Ink toxicity test 56
7.3.4 Isolation 57

Abbreviations

ALMA	Alginate methacrylate
BMM	Mineral medium Brunner
CAD	Computer-aided design
CA-HA	Carboxy-hydratropic acid
CA-IBU	Carboxy ibuprofen
CAM	Computer-aided manufacturing
CAT	Catalase
CEC	Compound of emerging concern
CFU	Colony forming unit
CL	Crosslinkers
CMC	Carboxymethyl cellulose
-COOH	Carboxyl functional group
COX	Cyclooxygenase
DNA	Deoxyribonucleic acid
EY	Eosin Y
FTIR	Fourier transform infrared
GPx	Glutathione peroxidase
GST	Glutathione S-transferase
GW	Groundwater
IBU	Ibuprofen
K_{ow}	Octanol-water partition coefficient
LC_{50}	Lethal concentration 50
LOD	Limit of detection
MA-SA	Methacrylic modified sodium alginate
MBR	Membrane bioreactor
MBRi3	Isolate no. 3
$-NH_2$	Amine functional group
NSAIDs	Non-steroidal anti-inflammatory drugs
OD_{600}	Optical density measured at 600 nm
-OH	Hydroxyl functional group
OH-IBU	Hydroxy ibuprofen
NGO	Non-governmental organization
NGS	Next generation sequencing
PCL	Polycaprolactone
POD	Point of departure
RNA	Ribonucleic acid
ROS	Reactive oxygen species
SDG	Sustainable Development Goals
SOD	Superoxide dismutase
SW	Surface water
synGW	Synthetic groundwater
synSw	Synthetic sewage
TEA	Triethanolamine
UN	United Nations
USA	United States of America
VC	N-vinylcaprolactam
VP	Vinylpyrrolidone
WWTP	Wastewater treatment plant
ι-CA	I-carrageenan

1 Introduction

For the last few decades there has been an increasing concern about the impact of anthropogenic activities on the environment. People are reminded all the time that the world is suffering changes never seen in the last centuries, for instance, climate change, pollution of water bodies and soil, the rise of sea level, severe recurring droughts, among others.

Often these events are first identified by the scientific community, which later urges society and governments to act. The United Nations (UN) is a good example of an organization that spreads these concerns to the public and appeals governments to change/create policies to solve or mitigate these issues. The recent UN‘s Sustainable Development Goals (SDG) is an ambitious project that compiles the major concerns society faces nowadays and prioritizes them according to their urgency and importance. The SDG’s sixth goal focus on “Clean water and sanitation”, which has also gained a lot of relevance lately, given the fact that water is one of the most crucial resources for humankind. Therefore, ensuring this resource does not get scarce is of utmost importance.

Around the world there are several water sources, unfortunately, the great majority do not meet the requirements to be used as sources of freshwater, which is the actual resource the agricultural, industrial and municipal sectors rely on. This resource is found in rivers, lakes, among other water bodies, being aquifers one of the main sources of freshwater [1], [2], denominated groundwater (GW) when found in geological formations. Surface water percolates through the soil due to its porosity or fractures and sinks until it reaches impermeable rock where it accumulates. This reservoir is called an aquifer. Depending on the composition of the soil layers through which the water percolates, a combination of physical, chemical, and biological processes occur, resulting in GW with distinct properties and high chemical and microbiological quality [2].

Nevertheless, GW is also a target of several threats that endanger its quality, such as, landfill leachate, surface sealing, topographic alterations, river canalization [3], salinity induced by irrigation, and contamination from septic tanks. [2], irrigated land with wastewater, among others. [4] Consequently, contaminants stemming from agricultural, industrial and domestic activity, such as pharmaceuticals, pesticides [3], fertilizers [2], heavy metals, bacteria [5] have been detected in GW. Besides anthropogenic activity, nature also plays a role in GW quality, for example through contamination from geogenic arsenic and fluoride [2], and saline intrusions. [5]

In cities, where more than half of the world’s population lives [3], population density and production of wastewater is considerably higher and harder to manage, this originates a concentration of contaminants that strike harder in GW’s quality, being these communities more susceptible to GW deterioration and scarcity of freshwater. Hence, neglecting aquifers might in consequence endanger the availability to freshwater for a great portion of the world’s population, somewhere around 1.5 billion city dwellers only. [6] Furthermore, exposing life beings to contaminated water sources can also have negative effects on their health, possibly extending these effects to humans by consuming aquatic organisms that live in contaminated waters. [7]

One might think that this problem is simply solved by treating GW before being provided to communities, but this might result as not so effective, especially if society continues to pollute water

bodies without restraints, keeping humanity in a cycle of polluting and then treat the polluted waters harming life beings in the meantime. From a holistic point of view a solution to this problem should tackle different steps along the water use process, such as, raise communities' awareness about the current problems and its consequences, develop new methods and adapt current ones as solutions to the problem, and above all, demand governments to approve policies that consider what is best concerning water usage and disposal, since governments are in the heart of directing society in the right path. [6] In turn, a sustainable use of GW not only provides freshwater for people complying with goal six from the SDG, but also goal two by contributing to a good nutrition and promoting a sustainable agriculture, goal nine through building a resilient infrastructure and goal eleven promoting more sustainable and resilient cities and human settlements. [2]

Thereby several projects arise searching for innovative solutions to tackle these issues, for example, MAR2PROTECT. MAR2PROTECT is a European Union project focused on the monitoring and preservation of GW, as well as raising communities' awareness about ways to protect GW quality and quantity. To achieve this goal the project aims to apply several methods of (bio)remediation, develop monitoring platforms, such as using artificial intelligence to detect any deviation that may threaten the GW safety and act accordingly and employ new-generation Managed Aquifer Recharge technology. The project is a collaboration of eleven partners, nine from seven European countries and two international partners, each one with its own investigation group and task. Each group has a different approach to achieve the main goal mentioned before and some of them also hold demo sites, which are specific locations selected due to its representative climatic conditions, type of GW pollution, political/societal context, among other factors. In these locations experiments on the technology and methods developed by the local team are also tested.

This master thesis was integrated into one of MAR2PROTECT's projects that focused on the bioremediation of contaminated GW with pharmaceuticals. The approach taken combined the degradation capacity of microorganisms with 3D printing to produce functionalized microbial frameworks that can be freely shaped and have different combinations of microbial strains distributed in distinct layers. The project can be divided into three stages: isolation of degrading strains/communities, implementation of said microorganisms into a 3D structure and evaluation of microbial degradation of targeted contaminants when inside the 3D structure.

The goals of this project are the following:

- Search for degrading strains/communities of a contaminant of interest
- Produce a print with biofilm similar properties
- Assess the communities/strains with better removal efficiency
- Evaluate the viability of employing the print in real GW conditions

2 Context and State of the Art

2.1 Threats to groundwater quality

GW can be found in a broad range of depths, from land surface to over 200 m, being 2 to 7 m the most common range from which GW is pumped [8]. Despite being shielded beneath the ground, GW is susceptible to anthropogenic activity from the surface. Several natural dynamics, such as the hydrological cycle, surface runoff and percolation, carry hazards laid by human hand on the surface that reach aquifers. Aquifers are particularly vulnerable to these hazards, as well as water bodies that depend on GW, namely, springs, wetlands and wells. [2] These changes can compromise GW availability as a resource for decades. [3] This scenario is especially concerning in cities, where rapid development and increasing demand is expected to continue in the next years. Consequently, not only it requires more freshwater to be delivered but also the negative effects are exacerbated, by increased pollution and waste management, compromising urban GW to be used as freshwater [9]. In places where rapid population growth has been observed, for instance China and India, wastewater is often discharged untreated because the building of infrastructure cannot keep with the demand, aggravating the risk of GW contamination. It is estimated that around 80% of global wastewater is discharged untreated. [3]

Amongst the threats GW is exposed to, contamination is probably one of the most complex of them all, due to the great variety of origins and compounds that can be associated to this activity, which are summarized in Table 1.

Table 1 | Major contaminants associated with agricultural, urban and industrial activity and their threats to GW quality. Adapted from [3]

Contaminant source	Potential contaminating compounds	Remarks on potential pathways and processes
Agricultural	Fertilizer (nitrates and phosphates) application as potential diffuse contamination	When nutrient load exceeds uptake capacity of plants, runoff or infiltration into GW bodies may result.
	Crop protection (pesticides, etc.) as potential diffuse contamination	Agrochemicals, and their degradation products, can runoff and/or infiltrate into and remain in GW bodies for substantial amounts of times.
	Use of veterinary products (antibiotics, hormones, etc.) as potential diffuse and point source contaminants	Antibiotics and hormones, although currently only detected in low concentrations GW, may pose a significant risk to the receiving environment.

Urban	Wastewater as potential vector for point source and diffuse nitrate and pharmaceutical contaminants	Wastewater may enter GW bodies through sewer leakage, poor infrastructure, or via receiving streams down-gradient of wastewater treatment plants.
	Runoff as potential vector for point source and diffuse nitrate, pesticide, road salts, etc. contamination	Products applied to urban surfaces readily leach into storm water and can reach GW at localized or diffuse infiltration points. In combined storm – sewer systems, untreated wastewater can also overflow as runoff.
	Leachate from solid and liquid waste as potential diffuse contamination	Lack of adequate lining of landfills or inadequate sanitation infrastructure can threaten aquifers through the introduction of solid and/or liquid anthropogenic waste as leachate.
	Managed Aquifer Recharge and wastewater irrigation as vectors for diffuse nitrate and pharmaceutical contaminants	In many water-scarce regions, wastewater presents a valuable resource. However, there is increasing concern regarding aquifers vulnerability underlying such systems, especially when these aquifers are considered as potential drinking water sources.
Industry	Spills and leaks as potential point source for BTEX (benzene, toluene, ethylbenzene, xylene) contaminants	Subsurface heterogeneities, even in relatively simple porous aquifers, with horizontal bedding features overlying aquitards, compose complex transport processes, posing a significant challenge for the remediation of BTEX spills.
	Runoff, leachate and precipitate as source and vector for diffuse contamination, and sever water chemistry alteration	Mining exposes minerals sulphates to surface reactions, resulting in radically altered pH conditions in associated waters. This phenomenon, known as acid mine drainage, may result in the precipitation or increased solubility of heavy metals.

2.1.1 Contamination by pharmaceuticals

For this project in particular, contamination by pharmaceuticals was the challenge focused on. Though pharmaceuticals have been present in human history for a long time, only after a few decades ago were these made more accessible to most people and a great variety of different pharmaceuticals produced. With time their consumption increased and today their use is widespread and produced on a large scale, due to their healing and disease preventive properties. On the other hand, from a few years ago persistent pharmaceuticals started being detected in several locations in the environment, giving rise to their new denomination as Compounds of Emerging Concern (CEC), because little is known about the risk they pose and their residence time in the environment. [10] But one thing is certain pharmaceuticals are designed to have a mode of action in the human body, and also resist harsh conditions, such as gastric acids, hence when present in the environment these compounds could also employ the same effect in other non-target living beings, for example animals, microorganisms and plants. [11], [12], [13] Furthermore, when resistant enough, these pharmaceuticals could prolong their effects for extended periods of time.

Recent studies start to show that, despite pharmaceuticals are in low concentrations in water bodies and do not cause any major damage to wildlife in the short-term, they might pose a bigger threat in the long-term by prolonged exposure, resulting in changes in wildlife's behavior and traits. [14] Moreover, the environment is hardly contaminated by a sole compound, but by a mixture of compounds, arising the possibility of the compounds potentiating the general toxicity of the mixture. [10]

Common sources of pharmaceuticals that end up in the environment are hospitals' waste, pharmaceutical industries effluents, landfill sites, diagnostic waste, research activity, wrong disposal of medicine and human and animal excretions. [4], [10], [11], [14] In turn, the most relevant ones are urban-sourced, such as, wastewater emission, combined sewer overflow, and leakages in wastewater infrastructure. [3]

In terms of pharmaceuticals consumption by humans and animals, when ingested these often do not get entirely degraded or assimilated. Therefore, part of the pharmaceuticals' compounds ends up in the excretions of the recipient, namely feces and urine, unchanged or as byproducts from its partial degradation. [14] In the case of humans, these excretions later undergo through several treatments in Wastewater Treatment Plants (WWTPs). WWTPs are designed to treat specific impurities, such as nutrients (carbon, nitrogen and phosphorus), pathogens and particulate matter, however, they do not account for emerging contaminants, thus they are not entirely removed from treated water. [4], [15], [16] Consequently, the presence of pharmaceuticals also hamper microbial activity, decreasing pharmaceuticals' removal rates. [15] The discharge of the treated effluents in water bodies, for example, rivers and seas, and treated sludge in crops fields carries with it the persistent compounds mentioned above. [17] Eventually, pharmaceuticals infiltrate in the soil, reach aquifers and contaminate GW. In turn, in the case of livestock, around 50-90% of the pharmaceuticals dose administered is excreted into the environment. Despite their excretions might undergo a similar path to human feces, it is also usual to use manure to fertilize fields, and when not accounted for, pharmaceuticals end up in the crops soil and it is only a matter of time until they

reach aquifers. Another scenario is the use of untreated manure, which is even worse because the number of contaminants, pathogens and nutrients is even higher, as well more concentrated, posing a higher threat to contaminate GW. [3], [13]

Nevertheless, the beforementioned issues lead governments to rethink their policies, and organizations to state their concerns so nowadays efforts are being made to mitigate and control pharmaceuticals emissions. For instance, in 2014 a report from the NGO CHEM Trust, among many suggestions, asked the pharmaceutical industry to accept responsibility for comprehensive environmental stewardship of its products and to develop green-by-design pharmaceuticals. [18] Also, since 2013 several European Union members have implemented collection programs for unused or expired pharmaceuticals, which would tackle the wrong disposal of pharmaceuticals. [19] Two years later, the European Commission went forward with its first watch list that included pharmaceuticals, promoting their monitoring and risk assessment. [18] Other countries, like the USA, has similar strategies, such as the Unregulated Contaminant Monitoring Rule established by USA's Environmental Protection Agency since 1996. It involves monitoring a number of contaminants and assessing their hazardous effects, which is revised every five years. Later, if justified, some contaminants are included in the Candidate Contaminant List, where further toxicological effects are assessed. Depending on the results, contaminants may then undergo regulation. [19]

Nowadays, there is a myriad of pharmaceuticals identified in GW ranging from non-steroidal anti-inflammatory drugs (NSAIDs), antibiotics, lipid regulators, beta-blockers, antiepileptics, stimulant, metabolites, among others. Some well-known compounds are IBU, salicylic acid, ampicillin, sulfamethoxazole, atenolol, carbamazepine and caffeine. Moreover most of these compounds can be found in sources that rely in GW, such as wells, springs, monitoring stations, all around the world. [4] Pharmaceuticals resistance to degradation together with their continuous influx into the environment are the major issues that contribute to their persistence and widespread detection. [15]

2.2 Ibuprofen

This project focused specifically on the compound IBU, which was already used in previous works developed by the project team. IBU, along with acetylsalicylic acid, paracetamol, naproxen and diclofenac, is one of the most used NSAIDs [13], [20] due to their antipyretic, analgesic, anti-inflammatory, and anti-blood clotting properties mostly used to relieve pain, symptoms of arthritis, rheumatic disorders, fever, degenerative disease, tendinitis, bursitis, sciatica, gout, and migraine. [11], [21], [22] These properties and its recognized safety, resulted in a high demand for this pharmaceutical, which has an estimated production of several kT/year world-wide [23], and the fact that is easily accessible (it's sold over the counter) potentiates the former statement. [24] It is such a relevant pharmaceutical that is listed in the Essential Drugs List of the World Health Organization. [12] Over the years, IBU has been accumulating in the environment until the point where nowadays it is considered to be a CEC. [9] To aggravate this situation, few policies to control or remove this compound from the environment have been practiced currently. [2], [16] According to Burri et al [3], no government or authority has established detection limits in drinking water for IBU. Unlike other

compounds, for instance, diclofenac. On the other hand, IBU is limited to 400 µg/L in drinking water, according to Australia's water supply guidelines. [25]

2.2.1 Detection of ibuprofen in the environment

A high consumption of IBU (dosage of 600-1200 mg/day) [23] and its excretion in human feces and urine is the main way IBU ends up in the environment, thus non-metabolized IBU and its conjugated and transformed compounds can be found all along the transport and discharge process of urban wastewater. [9], [22] In Table 2 it is described several locations where IBU has been detected as well as the respective concentration.
It is important to note that the distribution of IBU's concentration around the world is not uniform, because the presence of pharmaceuticals and their concentration in the environment is highly linked to the local population consumption patterns. [3]

2.2.2 Impact of ibuprofen in wildlife

The presence of IBU in several habitats for long periods has raised the concern whether its concentration and time of exposure could impact wildlife's health over time. It is not only important to assess the effects human activity has on the environment but also because this issue might escalate and become a public health problem. For instance, Nielsen et al. conducted a study with data from live births, stillbirths and miscarriages from North Jutland, Denmark, to assess the effects of NSAIDS consumption on gestation, they concluded these pharmaceuticals could lead to an increased risk of miscarriage. [24] In turn, this study was based on the fact that NSAIDs are consumed at doses ranging from 200 to 600 mg [24], which might not reflect the concentrations found in the environment. Nevertheless, in the scenario where IBU is left unattended and found in high concentration in drinking water this could lead to a generalized increased percentage of miscarriages around the location which is dependent on the same contaminated water source.
IBU's mode of action comprises a non-selective inhibition of both cyclooxygenase (COX) enzyme isoforms, COX-1 and COX-2, which in turn inhibits the synthesis of prostaglandin and thromboxane from arachidonic acid catalyzed by the mentioned enzyme. This interferes with the communication between cells by disrupting the autocrine and paracrine signaling, as well as the neural transmission and transport of ions across cell membranes, roles where prostaglandin takes part. [12], [20], [31] On one hand, inflammation and pain are reduced. [12] On the other hand, assimilation of IBU by wildlife can result in adverse effects and possibly harm them in unexpected ways, either because of the high dosage ingested or the period of exposure. In fish, prostaglandins are known to be involved in homeostatic functions in osmoregulation, immunity, reproduction and the hematological system, all possibly targets of IBU effects. [12]

Table 2 | Reported detections of IBU in the environment

Site sampled	Concentration (maximum)	Location	Reference
Groundwater	379 ng/L 293 ng/L 502.9 ng/L	Besòs River Delta, Besòs River, Llobregat River, Barcelona, Spain	[9]
Groundwater	0.018 µg/L (3.11 µg/)	47 sites across 18 states, USA	[26]
Groundwater	3 ng/L (395 ng/L)	164 sites across all Europe	[27]
Groundwater	n.d.-200 ng/L	17 well sites from a drinking water plant, Berlin, Germany	[28]
Groundwater	n.d.-0.6 ng/L	7 well sites, Hérault river basin, France	[29]
Surface water	n.d.-4.5 ng/L	3 river sites, Hérault river basin, France	[29]
Urban wastewater	2.23 µg/L; 12.61 µg/L	Universitat Autònoma de Barcelona, Bellaterra, Spain	[30]
WWTP	18-219 ng/L	2 effluents sites, Hérault river basin, France	[29]
WWTP	≤ 71.7 g/day -effluent 7.0-15.2 g/day - treated sludge	Terrassa, Spain	[17]

n.d. – not detected

Several studies have been conducted differentiating themselves by the organisms studied, the environments replicated, and the biomarkers evaluated in order to understand the mode of action and toxicity of IBU on life beings. For example, Saravanan et el. [22] exposed fingerlings of *Cirrhinus mrigala* to 14.2 ppm for 35 days and concluded that IBU might damage the fish gill's structure leading to hemolysis; interfere with the hemoglobin oxygen transport promoting more hemoglobin production resulting in a macrocytic anemia; activate an immune response with the release of lymphocytes; an increase of metabolic demands that resulted in a hyperglycemic condition, lower levels of plasma protein (probably used in the metabolism); disruption of the Kreb's cycle; and release of aminotransaminase and alanine transaminase into blood circulation, due to cell damage or disintegration.

In Gómez-Oliván et al. [11], *Daphnia magna* specimens were submitted to 2.9 mg/L of IBU for 48 h. Besides the determination of the Lethal Concentration 50 (LC_{50}), which describes the concentration of a compound that causes death in 50% of the study organism's population during the observation period, concluded to be 24.9 mg/L, it was observed that IBU increased reactive oxygen species (ROS) production disrupting the oxidative balance by increasing the activity of cytochrome 2 and interfering with the mitochondria activity resulting both in the production of the radical superoxide anion as a byproduct. Furthermore, IBU when in contact with the vasculature it acetylated the enzyme COX-2 promoting nitric oxide synthesis. The reaction between the latter and superoxide anion yielded a reactive nitrogen specie. The oxidative stress created by the reactive nitrogen specie and the superoxide anion resulted in the oxidation of proteins, which in turn promote mitochondrial dysfunction, leading to eventual irreversible damage, and loss of cellular ATP, jeopardizing the integrity of cells. It was also observed an increase in antioxidant enzymes activity, most probably as a countermeasure to mitigate the oxidative stress. Finally, in the study it was also noted that the oxidative stress stemming from IBU induced an increase in DNA oxidation resulting in its damage, and daphnid immobilization, indicating that the neural transmission associated to prostaglandin might have been disrupted.

Mathias et al. [12] tested several concentrations of IBU (0.1, 1, 10 µg/L) in *Rhamdia quelen* for 14 days. They observed an oxidative stress build-up by means of an increase in activity in glutathione peroxidase (GPx) and glutathione S-transferase (GST), as well as an increase in concentration in reduced glutathione, enzymes associated with antioxidant defense by ROS elimination. However, no DNA damage was observed in this experiment. Moreover, it was measured an increase in the branchial carbonic anhydrase activity, a crucial enzyme in the acid base regulation, respiration and ion uptake present in the gills of freshwater fish. This can be explained as a compensatory response to maintain the homeostasis. In turn, the observed increased plasma magnesium levels, probably due to reduced glomerular filtration in the kidney, and the inhibition of renal carbonic anhydrase indicated that IBU has a nephrotoxic effect in *R. quelen*. An immunosuppressive test was also conducted by the measurement of immune system cells, which resulted in the decrease of such cells in the presence of IBU predisposing *R. quelen* to diseases. Unlike what was observed by Saravanan, which observed an increase in immune response.

Parolini et al. [20] tested the cyto-genotoxicity of IBU in *Dreissena polymorpha* by exposing these mollusks to a gradient of concentrations (0.2-8 µg/L) for 96 h. It was observed that, although no DNA

fragmentation was detected, IBU was able to induce genetic injuries, as suggested by the increase in apoptotic cells and micronuclei. However, the authors mentioned that this genotoxicity might not be directly related to IBU itself but rather its metabolites and conjugates, which are known for being more toxic, and develop oxidative stress. Moreover, it was observed a disruption of the lysosomes' membrane stability of hemocytes and an increase in activity of three enzymes associated to the oxidative balance, catalase (CAT), superoxide dismutase (SOD), and GPx. The authors also found that even at the highest concentration, at the end of the experiment, these three enzymes activity returned to baseline levels, which indicated that the previous oxidative balance was reached, or the mollusks adapted to the new environmental conditions. Still concerning the enzymes, an increase in GST was observed, which functions in the detoxification of xenobiotics. The authors performed a Benchmark Dose analysis and found that the Point of Departure (POD) concentration for the majority of biomarkers studied was around the lowest concentration used (0.2 µg/L), except for SOD which yielded a value of 5.57 µg/L. This was explained by the presence of DT-diaphorase in bivalves, which protects the mollusk from the superoxide anion radicals, thus delaying an adequate response by SOD activity. Concerning CAT, GPx and GST the POD was below the lowest concentration, which indicates that IBU produces ROS quite fast, triggering a response from these enzymes to counteract ROS oxidation activity, therefore, IBU can be considered a main factor in inducing genetic damage through oxidative stress. In a nutshell, the authors state that at environmentally relevant concentrations IBU induces moderate cyto-genotoxic effects in zebra mussels.

In another study, David et Pancharatna [31] performed an experiment that consisted in exposing developing embryos of *Danio rerio* to a gradient of IBU concentrations (1-100 µg/L) for a period of 7 days. It was noticed that by increasing IBU exposure concentration the embryos mortality increased, and the hatching would take longer compared to the control without IBU. The larvae that would hatch in the presence of IBU also showed a decreasing heart rate, body mass, and length with increasing IBU concentration. Some of the larvae also showed growth deficiencies, such as pericardial edema, spinal curvature, irregular protrusion of the blastomeres to the exterior chorionic region, and deficient organization of tail bud, optic vesicle, brain, and somites. Furthermore, it was studied the fish response to stimuli, from 10 µg/L on the fish showed slow movements and did not respond to tactile or light stimuli. For the highest concentration (100 µg/L), besides the total lack of response to external stimuli, the pectoral fins were reduced to a lump of mesodermal cells, which corroborates the immobility of the fish submitted to this concentration and these only survived for a few hours.

With these few examples it is observable some of the effects of IBU on wildlife, which are not insignificant. However, a major issue of some studies is the assessment of non-environmentally relevant concentrations and short experiment duration, undermining the conclusions we may take from IBU effects.

2.2.3 Current methods to remove ibuprofen from water

No matter the contaminant present in GW, aquifers have some remediation measures themselves that attenuates the presence of pharmaceuticals, these normally consists in microbial degradation and adsorption to soil. However, adsorption only retards the contaminant transport since it is reversible, while degradation has a more important role in the actual contaminant removal. [9]

Nonetheless, these measures are not efficient enough for GW to be used as a freshwater source according to our current standards. Therefore, additional techniques must be applied to meet potable water requirements. In the course of time, several methods and technologies were developed to remove contaminants from effluents from anthropogenic activity before they reach aquifers. These approaches to treat other contaminants may also be adapted to remove IBU, in fact, this is already happening, and some applications are described in the literature. Some examples are displayed in Table 3.

2.2.4 Biodegradation of ibuprofen

In the previous chapter distinct techniques of IBU removal were illustrated. In this thesis a microbial degradation method was developed to remove IBU from GW. This is a simple method that requires finding degrading microorganisms and providing conditions as close to ideal for said microorganisms to metabolize IBU while inside GW. Biodegradation of pharmaceutical pollutants usually occurs in two ways, either by co-metabolism, where the pharmaceuticals are catabolized simultaneously with another compound, often denominated as non-growth-substrate and growth-substrate, respectively, by the same enzyme, or by substrate degradation, in which the pharmaceutical is assimilated and catabolized alone as a carbon and energy source. [14] The former one is the major responsible for IBU's degradation through microbes. [41] Furthermore, co-metabolism commonly does not result in complete degradation of the pollutant and may produce dead end compounds that are more toxic than the parent compound. Nevertheless, co-metabolism may be associated with microbial consortia where the product of one microorganism is the substrate of another, allowing the mineralization of the parent pollutant [41].

When considering the degradation of molecules by microbes, solubility, temperature, pH, salinity, molecule's pKa, among other factors, play an important role. [14] In WWTPs the higher the solubility of a molecule the higher is its accessibility to microbes to degrade them, however, it is also more probable for compounds to bypass the biological processes and end up in the effluent intact if not given enough time for degradation to occur. [15]

The solubility of compounds can be measured by the octanol-water partition coefficient (K_{ow}), which measures the compound's hydrophobicity. In a nutshell, the higher K_{ow} is, the higher is the compound's hydrophobicity, which translates to a lower solubility and higher adsorption to soil and suspended particles in water. These compounds are also called low-mobility substances. In general, high hydrophobicity compounds ($\log K_{ow} > 5$) adsorb more, resulting in more time for being degraded, hence they often have better removal rates. However, low solubility also means less accessibility of substrate to microorganisms possibly hampering the degradation rate. [9], [14] In turn, low hydrophobicity compounds ($\log K_{ow} < 2.5$) are well solubilized, hence more accessible to microorganisms, and the time available for their degradation is more similar to the hydraulic residence time of the wastewater. Depending on the conditions employed, not enough time is provided, thus their removal rate might be lower.[9], [14]

Table 3 | Tested innovative methods to remove IBU

Method	Example (medium tested)	Initial concentration	Removal duration	%Removal	Reference
Coagulation	Coagulation by aluminium and ferric sulphate (lake Roine; MiliQ water)	30-40 µg/L	1 h	<50%	[32]
Advanced oxidation processes	Photocatalysis by polymer coated with TiO_2 (aqueous solution)	100 mg/L	150 min	~40%	[33]
Adsorption	*Luffa cylindrica*/pyrrole composite (ethanol solution)	40 ppm	90 min	61.81%	[34]
Bacterial degradation	Ammonia oxidizing bacteria (tap water)	82 µg/L 915 µg/L	~20 h ~160 h	100%	[35]
Fungal degradation	White-rot fungi (culture media)	10 mg/L	3 h-7 d	70-100%	[36]t
	Fluidized bed bioreactor with *Trametes versicolor* (wastewater)	2.23 µg/L 12.61 µg/L	≤5 d 1 d	100%	[30]
	Stirred tank reactor with free pellets or immobilized white-rot fungus *Phanerochaete chrysosporium* (Kirk medium)	1 mg/L	50 d (continuous operation)	~100% (free pellets) >93% (immobilized)	[37]

	Fixed-bed reactor with immobilized white-rot fungus *Phanerochaete chrysosporium* (Kirk medium)	1mg/L	100 d (continuous operation)	~100%	[37]
Biodegradation	Membrane Bioreactor and conventional activated sludge treatment (wastewater)	14.6-31.3 µg/L	24 h	≥99%	[17]
Phytoremediation	*Populus nigra* L. (Murashige and Skoog medium)	0.03-30 mg/L	3 weeks	100%	[13]
Constructed wetlands	Vertical flow constructed wetland (wastewater)	8.3-17.2 µg/L	2 weeks	55-99 %	[38]
Enzymatic degradation	Crosslinked laccase aggregates (wastewater)	~31-34 µg/L;	6 h	≤5%	[39]
Filtration/ Adsorption	Sand filter (wastewater)	8.3-17.2 µg/L	2 weeks	49-90%	[38]
Filtration	Nanofiltration (urine)	14.5 mg/L	-	96%	[40]
Precipitation	Struvite precipitation (urine)	14.5 mg/L	-	>99.9%	[40]
Oxidation process	Ozonation (urine)	14.5 mg/L	-	~100% (<LOD)	[40]

LOD – limit of detection

IBU's log K_{ow} is 3.97, which is closer to high hydrophobicity, therefore is considered as a hydrophobic compound and usually is attributed to high removal rates in WWTPs. [14], [42] Conversely, it is also reported opposite information regarding the removal of high soluble compounds, mentioning that these have higher degradation rates, while low soluble compounds tend to be more recalcitrant. [15] Therefore, one may say that there may be a balance between solubility and degradation to obtain optimal results.

During IBU's degradation by microorganisms, intermediates might be formed. Usual byproducts comprise three isomers of hydroxy-ibuprofen (1'-OH-IBU, 2'-OH-IBU, 3'-OH-IBU), carboxy-ibuprofen (CA-IBU) and carboxy-hydratropic acid (CA-HA). [23], [41] Besides transformation, IBU may also undergo a conjugation reaction, for instance, with glucuronic acid. [20] According to Zwiener et al. [23] in aerobic conditions microbial degradation yields OH-IBU as the major metabolite, whilst in anaerobic conditions it is CA-HA. Regarding CA-IBU, it is found in both conditions.

When ingested by humans, 15% of IBU is excreted as the parent compound, 26% as the OH-IBU isomers and 43% as CA-IBU, conjugates and CA-HA, meaning that around 84% of the IBU ingested is not digested or assimilated by the human body, ending as a residue in wastewater. [10], [41]

IBU's intermediates are easily degradable and, therefore, do not reach high concentrations in solution. [41] According to Quintana et al. [41], it is possible to achieve a total mineralization of IBU using aerobic bacteria. This is supported by Goméz-Oliván et al. [11], stating that IBU is rapidly degraded under aerobic conditions with removal rates up 90%. In turn, Jurado et al. [9] states that IBU is more easily degraded in sub-oxic and nitrate reducing conditions in the GW, fomenting denitrification and aerobic respiration. According to Matamoros et al. [38], it is clearly observed that IBU degradation is greatly dependent on O_2 presence, necessary for aerobic respiration. Reinforcing this correlation between IBU degradation and aerobic conditions.

Even though IBU is degradable by biological means, it is important to lead its degradation until complete mineralization, due to its metabolites and conjugates higher toxicity compared to the parent compound [14], for example, the conjugate IBU diacylglycerol. [20] This can be tackled by adjusting the conditions where degradation takes place, yielding different metabolites and degradation rates. [10]

2.3 Bioprinting

One may think that the mere inoculation of degrading microorganisms into a targeted medium is solution enough for its treatment, despite its simple operation and control, this procedure has the disadvantage of needing to remove the microorganisms or disinfect the medium after treatment (requires an additional step and might turn out a hard effort). In turn, immobilized cells may be provided with a unique microstructure [43], have higher retention times [44], higher resistance to toxic shock, do not need high biomass loading, are easily separated [45] and may be reused for several cycles. [43] On the other hand, immobilized cells are normally associated with diffusive limitations for substrate yielding low growth/degradation rates compared to free cells. [45] Despite the latter drawback, the microbial degradation was coupled with bioprinting technology, by means

of incorporating the microorganisms inside a hydrogel. This method allows to produce a gel composed of various layers with different microorganisms, provide customized layers composition that better suit the requirements of the microorganisms, produce layers with different conditions (for example, a layer totally enclosed where low/no oxygen exists) and an easy solution to remove the microorganisms at the end of treatment, since these can be immobilized inside the gel.

Bioprinting is based on additive manufacturing technology, which consists in adding materials in a bottom-up layer-by-layer fashion. [46] The major feature of bioprinting is the precise positioning of proteins, growth factors, living cells, therapeutic agents, among other biomaterials, and spatial control of components, which changed the paradigm in clinical contexts, namely, tissue and organ engineering. [47], [48], [49] Bioprinting was soon associated with the advantage of possibly producing biomaterials that mimic the complex architecture and composition of organs, such as, heart, kidney and liver tissues. A harder endeavor to achieve by conventional tissue engineering methods. [46] Bioprinting brought improvements in this matter, but such goal was not achieved yet. [50], [51] As any early-stage technology there are some issues that require more research to better understand and optimize this technique. [52] Moreover, bioprinting allows to produce with relative ease heterogeneous living biomaterials integrating patient cells able to accompany the patient's growth, materials with high resolution geometric and mechanical complexity [53], render biomimetic-shaped 3D structures from medical images, for instance, magnetic resonance imaging and computerized tomography using computer-aided design and manufacturing (CAD/CAM) technologies, it is easy scalable [46], cost-effective [52], highly reproducible, and achieves an homogeneous cell distribution. [51]

Bioprinting features make this a promising technology for future development in areas, including drug screening, wound healing, angiogenesis, stem cell niches, physiological simulation and stimulate the rapid development of functional 3D tissues and organs manufacturing. [46], [50]

Several attempts to produce 3D bioprinted tissues are described in the literature, such as: an aortic valve conduit made of an alginate/gelatin hydrogel inoculated with porcine aortic valve interstitial cells and human aortic root smooth muscle cells; [53] a liver analogue construct with vascular-like network composed of rat hepatocytes and adipose-derived stromal cells incorporated in a gelatin/alginate/chitosan and gelatin/alginate/fibrinogen hydrogels, respectively; [50] a bilayer tube that mimics the arrangement and function of skeletal muscle tissue composed of mouse myoblast cells cultivated onto a polycaprolactone (PCL) nanofiber layer coated with an alginate methacrylate (ALMA) nanofibers layer. [54]

Another relevant area where hydrogel caught the attention of health professionals is the bioadhesives production. Hydrogels are ideal structures to maintain a moist-like environment around wounds, absorb tissue exudates, allow oxygen permeability [47], has good debriding properties and can absorb bacteria thanks to network expansion. [55] One such adhesive was developed by Stubbe et al. [55] , where a gelatin-alginate hydrogel was tested with human foreskin fibroblasts meant to stick to burn wounds and facilitate its regeneration. However, since neither pure alginate nor ALMA have skin adhesive properties, two possible solutions consist in oxidizing alginate and derivatives with aldehyde functional groups capable of forming covalent bonds with

free amino groups of tissue proteins [47] or produce a blend with other polymers with such properties, for example, gelatin, as described by the authors. [55]

Since the advent of bioprinting a variety of technologies were developed or adapted from other printing current techniques, bringing new approaches and improvements that further increased the potential of bioprinting in biomedical applications. Some common bioprinting techniques available today are based on inkjet, extrusion, stereolithography, and laser-assisted bioprinting. [51] Each technique has its particular pros and cons, therefore a certain technique is better suitable for some applications, where others are more limited. Next, the concept behind these methods [51], as well as some features of each one is described in Table 4 [46], [49], [50], [51], [52]:

- **Inkjet –** consists in dispensing picolitre droplets of bioink through a nozzle and depositing them onto a substrate [46], droplet by droplet this technique can produce intricate shaped structures with ease. Among inkjet techniques these distinguish themselves by the mechanism used to generate the droplet, including thermal, piezoelectric, and microvalve processes.
- **Extrusion –** involves dispensing a continuous filament of ink through a micro-nozzle in a layer-by-layer-manner. Different mechanisms may be used to dispense the ink, such as a piston, a screw, or pneumatic pressure. This is the most commonly used printing technique both in research and the commercial sphere. [52]
- **Stereolithography –** in this technique a substrate is immersed in a vat of bioink along with photoinitiations, which are molecules that crosslink the bioink, so it retains the desired shape. Layer by layer the liquid bioink is crosslinked via radiation in the UV-vis spectra, this process is called photocuring. After a layer is crosslinked, the substrate sinks one level, and a new layer is crosslinked and so on. This is a nozzle-free technique.
- **Laser-assisted bioprinting –** this technique is composed of three main parts: (1) a pulsating laser; (2) a donor-slide, containing the bioink coated with a thin layer of gold/titanium; (3) a receiver-slide, where the bioink is deposited. Briefly, a laser pulse is shot and oriented by a mirror, when it reaches the donor-slide a bubble is created through vaporization propelling bioink with it, then deposited onto the receiver-slide.

Still concerning the bioprinting methods features, although inkjet-based bioprinting is often linked with low cell viability there are reports of this method resulting in a print with >70% cell viability for chinese hamster ovary cells and primary rat hippocampal and cortical neurons. [49]

In turn, when extruding, parameters, such as the duration time, shear stress, syringe tip diameter, and non-physiological conditions, probably play a role in causing unexpected behaviors and damage to cells. [53], [56] Moreover, when increasing the extrusion speed, the previous parameters should be kept in mind, as increasing the speed also means increasing the shear stress applied on the nozzle's inner walls, submitting cells to rupture prone environment reducing cell viability. Nevertheless, extrusion usually has higher printing speed over jetting-based bioprinting.[46] Because of its features and simplicity, extrusion-based bioprinting was used in this project.

Despite each technique's features, bioprinting, in general, suffers from a major drawback that is the lack of mechanical strength and integrity of the printed structures due to the innate properties of

hydrogels. Where more focus has been applied for the development of new biocompatible materials taking into account mechanical properties, diffusion coefficient, biocompatibility and suitability with the printing process. [46]

2.3.1 Hydrogel

In 3D bioprinting there is a plethora of materials available to produce inks, the material dispensed by the printer. Common inks used in bioprinting consist of hydrogels made of polymers, including natural, such as alginate, gelatin, hyaluronic acid [53], collagen, agarose, cellulose [52], fibrinogen, and chitosan [50], and synthetic, such as poly(lactic acid), poly(lactic acid-co-glycolic acid), PCL, polyurethane, de novo designed peptides [52], poly(ethylene glycol) [47], and poly(vinyl alcohol) [48] polymers. A hydrogel may be composed of a mixture of different polymers and nanoparticles to yield a variety of new hydrogels that have distinct mechanical properties, functional groups for potential grafting, new functions, among other characteristics [47] In general, natural polymers have low mechanical properties and low tunable degradation rate and biological functions. In turn, synthetic polymers have high mechanical strength with tunable microstructure, despite lacking biological moieties. [48]

In this project an alginate-based hydrogel was employed. Attractive features of this material comprise its low cost, biocompatibility, biodegradability, low toxicity, low immunogenicity, high availability, a variety of crosslinking and biomolecular tethering flexibility, and immense exudate absorption. [53], [55] Thereby, alginate-based hydrogels are widely used in the biomedical area, for instance wound healing, drug delivery, cell transplantation, and tissue engineering, and have a very broad range of viscosities at room temperature, allowing for a more tunable and accurate bioprinting according to the application. [47], [53]

Alginate is a naturally occurring anionic polysaccharide usually derived from seaweed or bacterial biosynthesis using Gram-negative bacteria (for instance *Azotobacter* and *Pseudomonas* sp.). [47], [53] It is constituted by β-D-mannuronic acid and α-L-guluronic acid residues linked via 1,4-glycosidic bonds. Alginate is well-known to form ionic crosslinks between the carboxylic acid moieties and divalent cations, such as Ca^{2+}. However, the resulting gel has some drawbacks, including possible toxicity to cells at high Ca^{2+} concentrations [51], low elasticity, brittleness. and difficult control over swelling and degradation rate. [47] To overcome these limitations other crosslinking methods were developed, as well as the modification of alginate with functional groups that allow for more familiar, controllable and reactive bonds to be realized [47], such as the beforementioned oxidation of alginate with aldehyde functional groups.

Another common modification of alginate is the use of methacrylate groups, being the most frequent 2-aminoethyl methacrylate, glycidyl methacrylate and methacrylate anhydride. [47] This group of molecules usually substitutes the specific reactive residues of amine ($-NH_2$), carboxyl (-COOH), and hydroxyl (-OH) groups. [57]

Table 4 | Commonly used bioprinting techniques and its features. Images adapted from [51]

Bioprinting technique	Advantages	Disadvantages
Inkjet 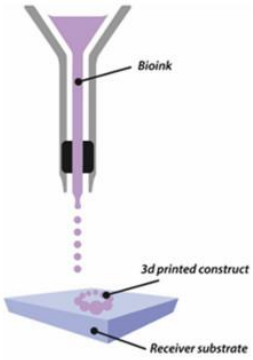	• High resolution (10-300 µm) • Capable of printing a singular cell per droplet • Accurate cell placement • Applicable into clinical settings • Adaptable for multimaterial printing • Low cost • Multiple cell/material delivery	• Prolonged processing time • Limited to low viscous bioinks (3-12 mPa·s) • Not suitable for large-scale 3D and over-hanging structures • High temperatures up to 300 °C (thermal-based) • Low thermal conductivity
Extrusion 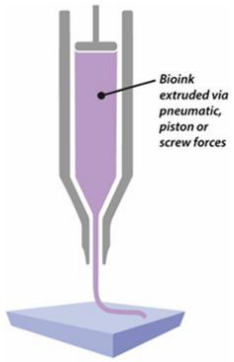	• Cell viability > 90% • Able to print highly viscous bioinks (30-6×107 mPa·s) and very high cell densities • Able to produce large structures • Applicable into clinical settings • Multiple cell/material delivery • Homogenous cell distribution	• Moderate resolution (200-1000 µm), compared to other methods • Critical timing of gelation time • Small diameter nozzles can lower cell viability
Stereolithography 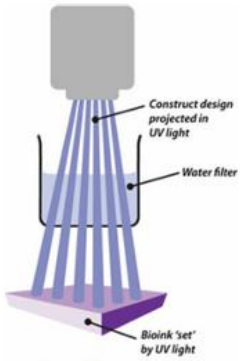	• High resolution (1-20 µm) • Fewer exposition to external stresses • High cell viability (>85%) • Low cost • No limitations of viscosities • Reduced fabrication time	• Possible entrapment of residual non-polymerized bioink • Possible harmful effects from photoinitiators and UV light • Induces oxygen inhibition
Laser-assisted 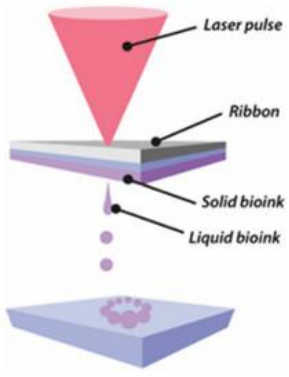	• High resolution (pico- to microscale) • Accurate multicell positioning • Nozzle-free, thus no clogging issues • Small printing volumes (pico- to nanoliter) • Reduced issues of shear stress	• Very expensive • Limited scale range • Heat from laser may damage cells • Complex design

Alginate modification with methacrylic anhydride is one of the most used, simple, and cost-effective methods to functionalize several biopolymers. [57] The corresponding reaction is summarized in Figure 1, and as observed methacrylic anhydride is substituted in the hydroxyl groups yielding ALMA. This reaction's efficiency may be increased when conducted in slightly alkaline pH (pH 8) and cool temperatures (4 °C), but if pH is too high then ester hydrolysis is induced. In turn, methacrylation degree can be controlled by the amount of initial methacrylate anhydride added. Moreover, the addition rate, agitation speed, temperature, pH, and other factors may play a role in the dispersion and reaction quality, hence yielding slightly distinct hydrogels. [47]

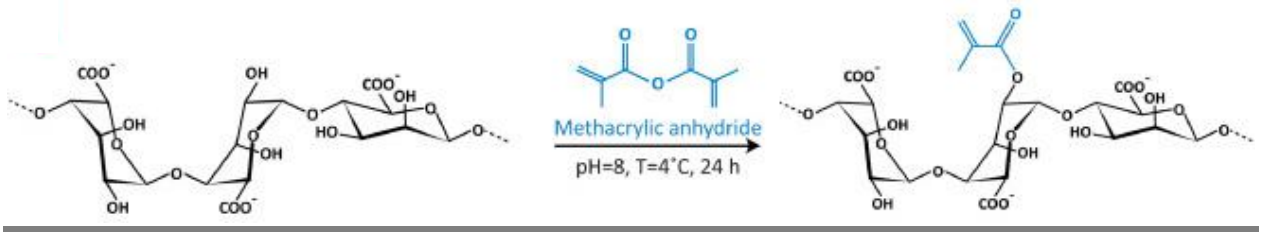

Figure 1 | Functionalization of alginate with methacrylic anhydride. Adapted from [46].

2.3.2 Crosslinking

Alginate modification alone is not sufficient to obtain a solid gel, thus it is usually followed by a crosslinking method. Crosslinking can be categorized in two ways, physical, when non-covalent interactions are made, therefore they are weak and transient, and chemical, when covalent interactions predominate, thus they are stronger and less easy to break. Crosslinking often occurs by chemical means and the polymerization reaction is started by a chemical agent or a light source, for example, the beforementioned ionic crosslinking of alginate by divalent cations was a chemical agent mediated crosslinking, although this is regarded as a poorly controlled process and the resulting gel has limited long-term stability due to the release of these cations into the surrounding media. [47]

Other promising crosslinking techniques have gained emphasis in current crosslinking procedures, such is the case of photocrosslinking. This method involves the use of radiation on the UV-Vis spectra capable of producing highly reactive free radicals, consequently these free radicals start the polymerization between the functional groups of polymer chains. Depending on the photocrosslinking performed a photoinitiator might be required, these molecules absorb light photons and convert light energy into chemical energy, thus helping in the polymerization reaction but do not take part in the polymerization itself. [57] Conversely, functional group sustained photocrosslinking facilitates bulk polymer crosslinking, photoimmobilization, surface modification, molecular labelling, and particle fabrication. Furthermore, its highly selective, efficient, and does not produce toxic or reactive products. [57] Unlike chemical crosslinking, photocrosslinking is straightforward, fast, cost effective, and may afford better spatiotemporal control over gelation and tissue mechanics while not limiting the possible printing time, made possible by adjusting the incident beam coordinate, light intensity, and exposure time. [47], [48], [53], [55] But what really makes photocrosslinking attractive it's the non-invasive and capability of in situ

photopolymerization, as well as promoting the search for new moieties in natural polymers to ease the method itself, which uncovered ways to change and improve mechanical properties of hydrogels. [57]

There are two well-known ways of photocrosslinking ALMA chains. When alginate is methacrylated a carbon-carbon double bond is present in the grafted molecule, that under UV light easily undergoes free-radical polymerization with amine, carboxyl and hydroxyl functional groups, resulting in ALMA chains crosslinking. This method besides simple, it is not affected by environmental conditions, such as pH and temperature, thus being a stable reaction, The crosslinking degree, and consequently mechanical properties are dependent on the number of methacryloyl substitutions. [57] However, this method relies in UV light, which it is known for generating ROS that might induce endogenous oxidative damage to DNA, hampering cells' viability, and cause accelerated tissue aging or cancer, this is disadvantageous for the biomedical field where cells and biomaterials are used in most, if not all, its applications. [48]

Thereby, other techniques rely in visible light, which is less harmful for biologic materials, can penetrate tissues at higher depths, and there is a broader and cheaper market for visible light sources [48], [56], for instance EY, tris (2,20-bipyridyl) dichlororuthenium (II) [57], camphorquinone, fluorescein, and riboflavin [48] are some photoinitiators activated by visible light. Specifically for EY, this molecule is excited between 450-550 nm [57] and another component, denominated coinitiator, capable of electron transfer [58] is necessary for a successful crosslinking. Usually, this role is carried out by amines, including TEA. [58] Both EY and TEA participate in the radical generation process at reactive moieties of the polymers, though EY is the actual initiator, while TEA helps EY produce radicals. [56]

Briefly, under visible light EY gets excited through a singlet to a triplet state (Figure 2, (1)), though the latter is the most relevant for the polymerization due to its longer lifetime, allowing enough time to react with TEA. The excited triplet then extracts an electron from TEA forming radical-cation/radical-anion pairs (Figure 2, (2)), held together by electrostatic attraction. Then ion transfer, mediated by protons (H^+), results in a pair of neutral radicals, now able to diffuse apart (Figure 2, (3)) [58]. Finally, TEA radicals react with the polymers' functional groups, such as methacryloyl groups in ALMA [48], yielding new radicals now able to react with other polymer chains' functional groups (Figure 2, (4)), this way initiating the actual crosslinking. Regarding the EY radicals these do not take part in the functional groups' radicalization, instead it is believed to act as radical chain terminators or undergo other reactions leading to its bleaching. [58] To further increase the speed of the radical generation co-monomers with vinyl groups, including N-vinylcaprolactam (VC) [48], poly (ethylene glycol) diacrylate, and vinylpyrrolidone (VP) might be also added. [57]

During this reaction, EY is the reaction catalyst, hence does not get consumed, conversely TEA and VP are consumed. This process can be monitored by the color transition from red to yellow, which occurs after formation of activated EY (Figure 3, A). It is important to note that for low initiator and co-monomers concentration these molecules may determine the hydrogels mechanical properties due incomplete gelation, however, after a threshold the hydrogel's mechanical properties are mainly dependent on its polymer and reactive moieties and not the crosslinking components. [48]

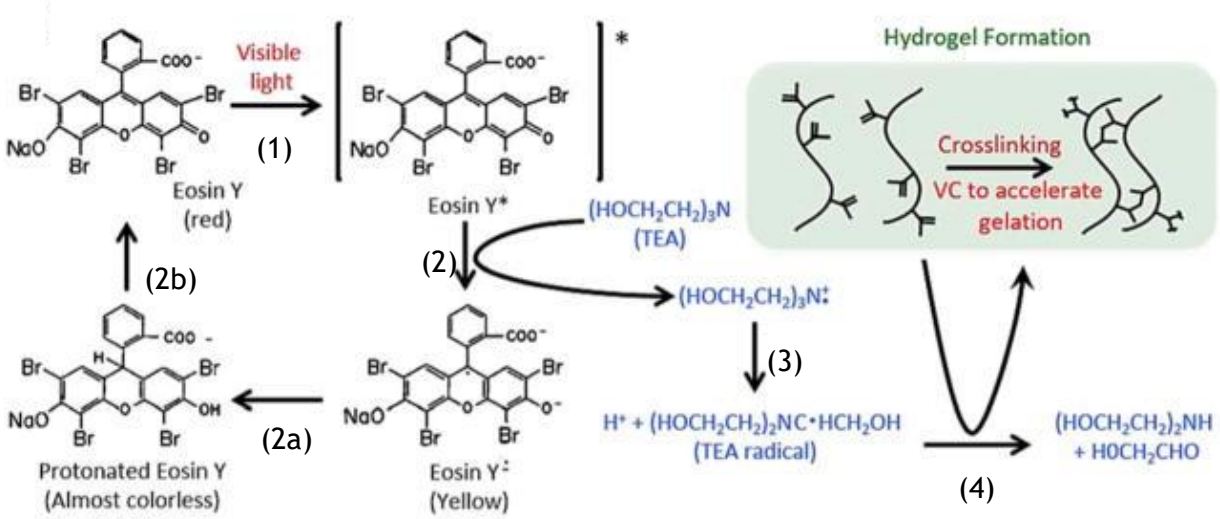

Figure 2 | Key steps of the photoinitiation mechanism of free radical polymerization by EY/TEA system. Adapted from [47].

Gels crosslinked through this method besides having reduced risk by using visible light compared to UV, it also allows to produce stable gels for a long period of time (18 months), making this a great solution for biomedical applications. Nevertheless, TEA usage should be done within reasonable limits, since high TEA concentrations can cause undesirable cytotoxic effects on some sensitive cell types. [57]

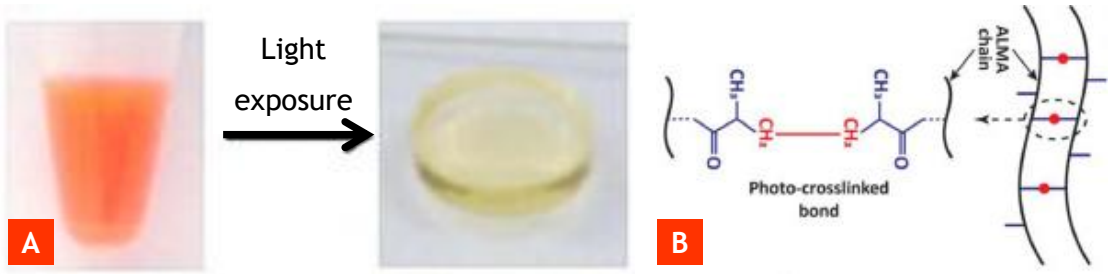

Figure 3 | (A) Color change of EY induced by visible light. Adapted from [47]. (B) Bond established by ALMA polymer chains after photocrosslinking. Adapted from [46].

2.4 Aim

This study aimed at assessing the ability of two previously isolated bacterial consortia from wastewater to degrade IBU and isolate the members of these consortia responsible for IBU degradation. Then apply the consortia and the degrading strains into an alginate-based hydrogel, followed by 3D printing the hydrogel with extrusion to produce a 3D structure, solidify the 3D printed structure through an EY/TEA-based photocrosslinking and evaluate IBU degradation performance.

3 Materials and methods

To test the approach pursued the laboratorial work can be divided into 4 stages. First, the degrading microorganisms were grown (chapter 3.2); second, the ink that will incorporate the microorganisms was prepared; third, the ink was inoculated and printed by extrusion (chapter 3.3); finally, the 3D printed gel was tested in GW-like conditions (chapter 3.4). In addition, strains from a membrane bioreactor (MBR) consortium previously recovered from wastewater were isolated and tested for their ability to degrade the target pollutant (Chapter 3.5).

3.1 Media preparation

3.1.1 Mineral medium Brunner

Mineral Medium Brunner (BMM) is a defined medium lacking a carbon source, which in this project was chosen to be IBU and was added later in the experiments. BMM was prepared according to DSMZ recipe 457 (appendix 7.1).

3.1.2 Ibuprofen stock solution

IBU stock solution of 10 g/L was prepared by dissolving ibuprofen sodium salt in distilled water. After vortexing thoroughly, the solution was sterilized by passing it through a 0.22 µm filter. The stock solution was stored at -20 °C.

3.1.3 Synthetic sewage

To complement the addition of IBU, a solution of synthetic sewage (synSw) was also added between 1-10%, prepared according to [59]. This solution allowed the microorganisms to grow faster, otherwise the time needed to grow them would simply be too long. The synSw was composed of the compounds described in Table 5 and dissolved in distilled water. At the end the pH of the solution was adjusted to 7.5±0.5.

Table 5 | Composition of the synSw solution

Reagent	Quantity
Peptone	16 g/L
Meat extract (or comparable vegetable extract)	11 g/L
Urea	3 g/L
Sodium chloride (NaCl)	0.7 g/L
Calcium chloride dihydrate ($CaCl_2 \cdot 2\ H_2O$)	0.4 g/L
Magnesium sulphate heptahydrate ($MgSO_4 \cdot 7\ H_2O$)	0.2 g/L
Potassium monohydrogen phosphate anhydrous (K_2HPO_4)	2.8 g/L

3.2 Cells cultivation

During the project two different consortia were used, namely MBR2 and MBR5, which were obtained by a group member through refinement of the bacterial community from wastewater.

Fresh cultures in nutrient rich medium were always prepared prior printing usually in two replicates. First a pre-culture was performed from cryostocks and after incubation a new culture was prepared from the pre-culture. When the end of exponential phase was reached cells from the culture were inoculated into the ink that would be printed. This allowed the bacteria to adapt to the new conditions of the ink, resulting in higher IBU degradation.

3.2.1 Incubation

The pre-culture and culture media formulations are described in Table 6 . During the cultivation, the cultures were incubated at 25 °C, 120 rpm, and usually for 20 h. The OD_{600} was measured regularly on a spectrophotometer (BioTek Synergy H1, Agilent, USA) at 600 nm.

Table 6 | Composition of the culture media

Reagent	**Quantity**	
	Pre-culture	Culture
BMM	Until 4 mL	Until 30 mL
synSw	10%	1%
IBU	10 mg/L	10 mg/L
Cells	100 µL cryostock	Preculture needed to achieve OD_{final} of 0.5

3.3 Bioprinting

The main compounds that take part in the gelation process were: methacrylic modified sodium alginate (MA-SA), the polymer's substrate; ι-carrageenan (ι-CA), a stabilizer agent; carboxymethyl cellulose (CMC), a structure agent; EY; and TEA. The last two are from now on called cross-linkers (CL) due to their function in making the MA-SA chains bind with each other and produce a mesh. The solvent used was BMM with synSw as prepared in Table 6. Finally, the bacteria to be tested were added to the mixture, which was skipped for the negative control.

3.3.1 Methacrylic modified sodium alginate preparation

For MA-SA production sodium alginate was dissolved in water to a concentration of 2% w/V at 80 °C and 700 rpm. Next, the solution was cooled down to 4 °C and kept stirring on ice, while a volume (in mL) of methacrylic anhydride 20x the mass (in g) of sodium alginate was added to the solution, followed by a pH adjustment with 5 M NaOH poured dropwise until pH 8. Afterwards, the solution was incubated at 4 °C and 800 rpm for 72 h.

During the incubation period the solution slowly turned into a mixture of a filamentous white solid, which corresponds to the MA-SA product, and a liquid phase. After incubation, MA-SA was washed by adding ethanol to a proportion of 1:1 and centrifuging (Centrifuge 5804 R, Eppendorf, Germany) at 9000 rpm, 4 °C for 10 minutes. The Falcon tubes were left slightly open so the methacrylic anhydride could evaporate. The supernatant was discarded, and the washing procedure repeated at least three more times. Next, the MA-SA pellets were slightly grinded and let dry over 24 h for the ethanol to evaporate.

In order to keep consistency between batches, two quality control tests were performed on the yielded MA-SA. First, its cross-linking ability was tested in conditions comparable to the printing procedure (chapter 3.3.2 and 3.3.3). Secondly, the spectrum of different batches was measured on a Fourier Transform Infrared (FTIR) Spectrometer (Cary 630 FTIR Spectrometer, Agilent, USA) and compared with previous measurements.

3.3.2 Ink preparation

Rich medium, BMM with 1% synSw, was pipetted into a beaker and 1.8% w/V of MA-SA added, then the mixture was dissolved entirely at 80 °C and 300 rpm and covered to prevent the solvent from evaporating. When a homogenous solution was obtained, 1.3% w/V of ι-CA was added and dissolved at 80 °C and 700 rpm. Finally, CMC was added at 1.5% w/V and mixed at 80 °C and 900 rpm. After total dissolution the ink was let to cool down to 40 °C and stored at 4 °C for up to 2 weeks. In order to work as close to sterility all the reagents were added inside a biosafety hood and the solution covered at all times.

Right before printing the CL are added to the previous ink, due to their photo sensitivity. First, the ink was transferred to a syringe and 5 mL of ink were extruded into a container (for example 6 well-plate), then the bacterial cultures were added to individual containers with ink to a final OD_{600} of 0.5. From this step on, more caution was required, as the next reagents might be toxic. 5 µL/mL of gel of 0.5% EY in VP and 50 µL/mL of gel of 5 M TEA in 0.1 M HEPES buffer were added, respectively. Finally, the finished bioink was transferred to a syringe and from there to a cartridge with two plungers through its tip, thereby minimizing the amount of captured air bubbles in the cartridge. Finally, a cap was attached to the cartridge and stored in a sterile falcon.

3.3.3 3D-bioprinting

The cartridge was mounted onto the 3D printer (3DDiscoveryTM Evolution Bio-printer, RegenHU, Switzerland). When starting the printer, first the needle size was measured by the machine and the coordinates adjusted to the tip's extremity. The origin, coordinates (0,0,0), were manually adjusted so the tip was close to the microscope slide. Finally, the applied pressure was adjusted so the ink was dispensed in a straight line without curling on the tip. Then the script containing the design specifications (chapter 3.3.4) was run and the 3D object printed onto a microscope slide. When finished the 3D object was photo-crosslinked under green light (520 nm) for around 10 minutes and stored on the microscope slide in a Falcon tube to preserve sterility.

3.3.4 3D object computer-aided design

To produce the 3D object's design the BioCAD (RegenHU, Switzerland) program was used. Here a 7 mm radius circle with 5 layers and a layer height of 0.35 mm was designed. For the filling an offset of 0.1 mm, a line spacing of 1.2 mm, and a rotation angle of 30° were used, this determined how far the filling was dispensed from the border, the gap between each new filling line, and the rotation a new layer was formed from the one it preceded in clockwise direction, respectively. While printing, the velocity the ink was dispensed at, also called feed rate, varied according to the ink's characteristics, although 13 mm/s was a standard value.

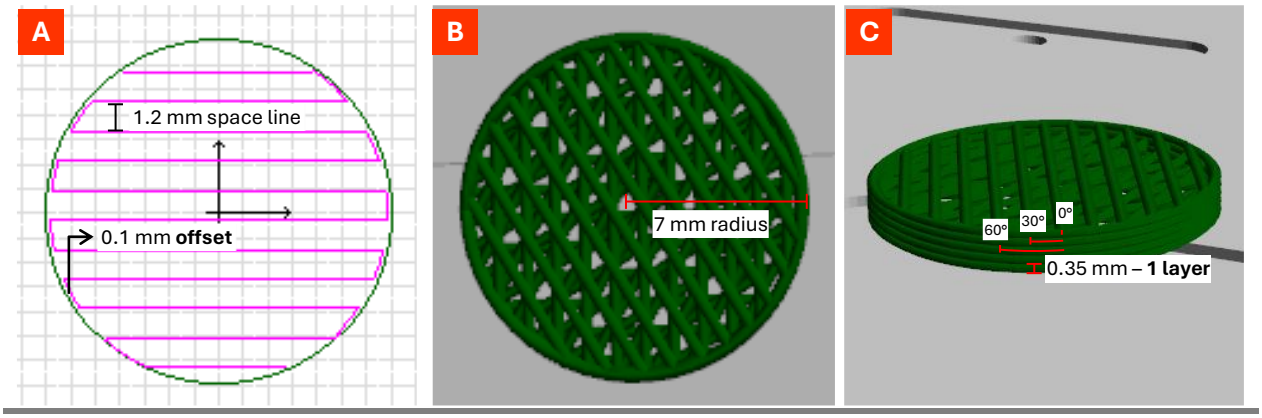

Figure 4 | Entered dimensions to print the bioink. In C the increasing degrees exemplifies how the starting point of printing changes for each new layer.

3.4 Degradation experiment

The following experiment aimed to evaluate ibuprofen degradation performance of the bacterial consortia and strains inside a 3D-printed gel, the viability of applying a printed gel to the target water bodies, and the adverse effects of this approach, such as leaching of cells to medium, and decrease in degradation performance.

To simulate GW-like conditions, flasks were prepared with 30 mL of either surface water (SW), from a demo site of another group member of MAR2PROTECT, or synthetic groundwater (synGW), made in the lab, then inoculated with around 1 mL of 3D printed gel with the bacteria incorporated. One of the performed controls was a cell free gel, called non inoculated gel (nin gel), meant to understand the effect the gel might have on the concentration of IBU over time. And other two controls had cells in suspension either in poor medium, synGW or SW, or in rich medium, BMM with synSw, meant to be the worst- and best-case scenario for cell growth, respectively. For the two last controls a volume of cell culture was pipetted to obtain a final OD_{600} of 0.5 in 1 mL, so it is comparable to the OD_{600} inside the gel. Three replicates were performed for each condition, twelve in total. Later these were incubated at 25 °C and 120 rpm.

As observed in chapter 2.2.1, IBU's concentration in the obtained SW was similar to those in the environment and was measured to be too low to be detected by a HPLC. Therefore, all solutions were spiked with IBU to a final concentration of 10 mg/L.

Over time the cultures and controls were sampled to measure the cell growth and the concentration of IBU through a spectrophotometer and a HPLC, respectively.

3.4.1 Optical density measurement

During the experiment, OD_{600} was measured regularly on a spectrophotometer (BioTek Synergy H1, Agilent, USA) at 600 nm, in order to understand how fast and well the cells grew inside the medium in bulk.

3.4.2 High performance liquid chromatography

IBU's concentration was monitored using a HPLC method. First, the sample was extracted to prevent clogging or damaging the column. An HPLC system from Agilent Technologies (USA) was used with a degasser, pump, and diode array detector from the 1260 Infinity technology, while the autosampler and column handler were from the 1200 Series technology. A Zorbax SB-C18 4-Pack (P.N. 820950-920) column was used.

The chromatographic separation was conducted using the column at 35 ºC, and two mobile phases, being ultrapure water with 1% of formic acid as mobile phase A and HPLC grade methanol as mobile phase B. The flow rate was set to 700 µL/min. The mobile phase's gradient was programmed as follows: (1) 0 min, 20% B; (2) 2 min, 95% B; (3) 7 min, 95% B; (4) 9 min, 60% B. The injection volume was 10 µL, and the IBU was measured at 230 nm.

3.4.3 Extraction protocol

The procedure to remove debris from the samples, such as cells, gel fragments or particles present in the SW, consisted in centrifuging the samples for 10 min at 21300 rcf and 4 ºC in a centrifuge (Microcentrifuge 5425, Eppendorf, Germany), then mix the supernatant 1:1 with chilled methanol, vortex the mixture and incubate for 15 minutes at 4 ºC. The centrifugation step was repeated and a HPLC vial filled with the supernatant.

3.4.4 Ink toxicity experiment

This experiment was designed to evaluate the ink components' effects both in cell growth and IBU degradation rate. Similarly to chapter 3.2, this involved adding a sole ink component to either MBR2 or MBR5 consortia and incubate them. A culture with only bacterial consortium and a flask with only medium were also prepared as controls. Two replicates were performed for each condition, sixteen in total. The composition of the different cultures is shown in Table 7.

Table 7 | Composition of the different media to test the effects of the gel components in the cells' performance

Sample name	BMM[1] (mL)	%synSw	IBU (mg/L)	Cells (OD_{final})	MA-SA (mg)	I-CA (mg)	CMC (mg)	CL (mg/L)
Abiotic control	45	1%	50		-	-	-	-
BMM control	45	1%	50	0.05	-	-	-	-
MA-SA	45	1%	50	0.05	810	-	-	-
I-CA	45	1%	50	0.05	-	585	-	-
CMC	45	1%	50	0.05	-	-	675	-
CL	45	1%	50	0.05	-	-	-	50 (TEA) 5 (EY)

[1] Filled up until specified volume.

Since only the CL are activated by green light, only its corresponding cultures were exposed to green light for 10 minutes as if it was a normal ink.

The cell growth was monitored by measuring the OD_{600} of the culture as mentioned in chapter 3.4.1, and the IBU concentration by HPLC as mentioned in chapter 3.4.2.

3.4.5 Survival test

A usual degradation experiment would take multiple weeks, which gave rise to the question of whether the cells were still surviving inside the 3D printed gel. With that in mind, either a small piece of gel, later crushed inside the medium, or 100 µL of liquid, in case of the cells suspended in poor medium, were inoculated in 30 mL of BMM with 1% synSw and 50 mg/L of IBU. Followed by incubation at 25 °C and 120 rpm. Such high IBU concentrations were used to ensure the carbon source was not limited. Up to three replicates were performed for each condition, seven to nine in total. The cell growth was monitored by measuring the OD_{600} of the culture as mentioned in chapter 3.4.1, and the IBU concentration by HPLC as mentioned in chapter 3.4.2.

3.5 Strain isolation

3.5.1 Plate isolation

Solid plates were prepared according with the methods described in chapter 3.2, with 1% of synSw, 15 g/L of agar, 0.5 mg/L of yeast extract and 10 mg/L of IBU dissolved in BMM. When dried, 100 µL of MBR2 culture were spread with a Drigalski spatula into two plates and incubated at 25 °C. Next, strains were isolated by picking the grown colony forming units (CFU) and then inoculated in duplicates with the quadrant and cross streaking methods in new plates, followed by incubation at 25 °C. Next, the isolates were grown in liquid cultures as described in chapter 3.2, apart from one isolate. Two replicates were performed for each isolate, sixteen in total. The cell growth in the liquid cultures was monitored by measuring the OD_{600}, and the IBU concentration by HPLC as mentioned in chapter 3.4.2. Finally, cryostocks of the isolates were prepared in 40% glycerol and stored at -80 °C.

3.5.2 Dilution “isolation”

The approach taken in this method aimed to find the highest dilution where IBU degradation could still be observed, implying the reduction of complexity of the consortium with each step and expecting that cells growing in these conditions would consist of the ones that take more advantage in degrading IBU. A serial dilution of the MBR2 consortium was performed with 10x step dilutions up to 10^{-6}. 100 µL of dilutions 10^{-3}, 10^{-4}, 10^{-5}, and 10^{-6} were used to inoculate fresh liquid medium and grown as mentioned in chapter 3.2. Two replicates were performed for each isolate, eight in total. The cell growth was monitored by measuring the OD_{600} of the culture as mentioned in chapter 3.4.1, and the IBU concentration by HPLC as mentioned in chapter 3.4.2.

In addition, the composition of the resulting cultures was assessed by 16S rRNA gene sequence-based analyses performed by a colleague. The DNA was isolated using the ZymoBIOMICS DNA Miniprep Kit (ZymoResearch, Irvine, USA) according to the manufacturer’s instructions. The V4 region of the 16S rRNA gene was sequenced (primer sequences 515f “GTGYCAGCMGCCGCGGTAA” and 806r “GGACTACNVGGGTWTCTAAT”) using the Quick-16S Plus NGS Library Prep Kit (V4)

(ZymoResearch, Irvine, USA) to create a DNA library. The library, containing 4 pM DNA (spiked with 25% PhiX), was sequenced in-house on a MiSeq platform (Illumina, San Diego, USA), following the manufacturer's instructions. Raw reads were processed using the R library dada2. This involved quality control steps including analyzing primer sequences, assessing error rates (maxN = 0, maxEE = c(2,2), truncQ = 2), and identifying chimeras A phyloseq object was then created using the phyloseq R library. This object consisted of an amplicon sequence variant table, a taxonomy table, and sample data.

3.6 Statistical analysis

A statistical analysis was performed to objectively verify whether the results obtained showed any difference between the tested conditions and controls, as well as among distinct conditions. The average values over time of each condition were analyzed with the Mann-Whitney U test and a significance level (α) of 0.05 using the statistical program R. Results with P values below 0.05 were considered statistically significant. No statistical analysis was performed for the ink toxicity results of the IBU degradation, due to few datapoints acquired, the sequence analysis, and MBRi3 cell growth, due to no comparison can be done.

4 Results and Discussion

4.1 Consortia

4.1.1 Degradation experiment

The following experiment assessed the growth and degradation performance of the bacterial consortia MBR2 and MBR5 inside a 3D printed gel (Figure 5). At first glance, all batches between the first and second timepoint did not demonstrate any change, which was indicative that the consortia were still adapting to the new environment, for example by producing the required proteins to survive of IBU metabolization. After 94 h of incubation, IBU's concentration for the bulk in BMM of both consortia significantly decreased (P-value<0.05), indicating IBU was being metabolized. MBR5's bulk in synGW and 3D printed gel began degrading IBU at a later stage, however, MBR5's gel still significantly reduced IBU concentration within two weeks compared to the nin gel, whereas for the bulk in synGW this reduction was not significant (P-value>0.05). Regarding the nin gel, the 3D printed gel itself appears to have no effect on IBU over time, as expected. In terms of MBR5's 3D printed gel and bulk in synGW, at the beginnig the print seemed to be performing worse than its bulk counterpart, however, after around 300 h this tendency ceased and the 3D printed gel appeared to begin degrading faster. However, the statistical analysis indicats there was no singnifcant difference between these two samples (P-value>0.05): Indeed, the size of the error bars should be taken into account, as they indicate a high flucuation of the values. In turn, when comparig with the bulk in BMM, MBR5's 3D printed gel was able to metabolize IBU below detectable levels as well, although at a much slower pace (P-value<0.05), evidencing possible diffusion limitations decreacsing the degradation rate. When looking at both bulk in BMM, MBR2 seemed to have a slight advantage against MBR5 in degrading IBU in a shorter time , although this is not supported by the statistical analysis (P-value>0.05).

In a nutshell, the positive controlsperfom better in general compared to the other cases, hence the rich medium plays a role in enhancing the IBU degradation perfomance. On the other hand, the consortia inside a 3D printed gel composed of rich mediuim did not perform significantly better than when is in a poor medium as liquid culture, probably due to limitations associated with the gel.

Further experiments were performed with the MBR2 consortium, because MBR2 seemed to be faster degrading IBU than MBR5. Figure 6 comprises the results of a new degradation experiment performed with MBR2 in a SW, instead of synGW. Similarly to the previous figure the bulk in SW and the 3D printed gel experienced an initial lag phase and started metabolizing after 84 h. Conversely, the bulk in BMM, unlike previously, appeared to metabolize IBU from the beginning of the experiment bypassing the lag phase. The nin gel in this experiment did not behave as expected, IBU somehow was consumed over time, but unlike the previous medium, which was autoclaved before being used, the current SW was a nonsterile water sample, thus containing a plethora of live organisms and probably they were used to survive in water containing IBU, consequently the SW's organisms, where the nin gel was inoculated, might have caused these results.

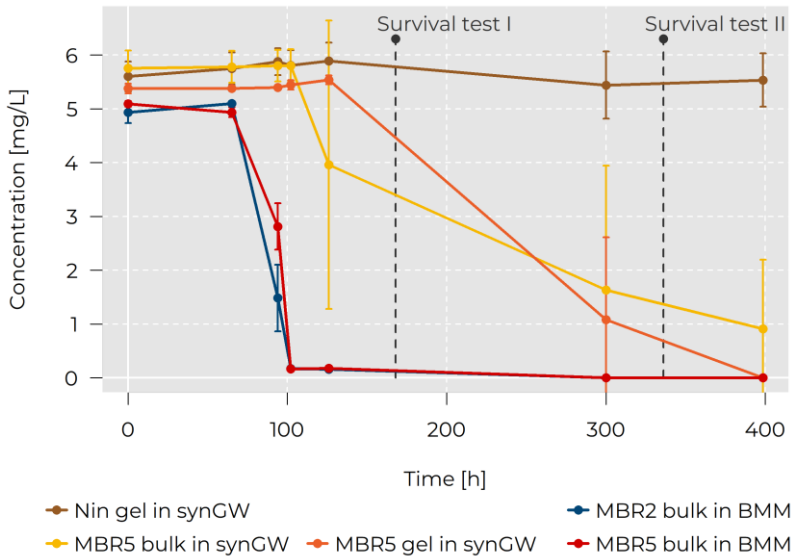

Figure 5 | IBU degradation experiment by MBR2 and MBR5 consortia represented as the change of IBU's concentration over time. Experiment carried out with inoculation of MBR2 from a liquid culture to a rich medium, denoted as BMM (**dark blue**). And MBR5 inoculated inside a 3D printed gel (**yellow**) in synGW and corresponding controls, inoculation of MBR5 from a liquid culture to synGW (**orange**), and to a rich medium, denoted as BMM (**red**). In **brown** is represented the nin gel in synGW. Further information about when the survival tests, derived from this experiment started, is shown in **gray**. Values plotted are means ± standard deviations for three independent cultures.

Moreover, the experiments conducted in SW resulted in the fragmentation of the 3D printed gels into tiny pieces over time until there was no gel visible (appendix 7.2). At around 1 week the 3D printed gel would start to fragment at a fast pace, after which it can almost be considered as its bulk counterparts. This is probably explained by the presence of unknow microorganisms capable of degrading some of the hydrogel's components leading to its fragmentation. The bulk in BMM, once again, seemed to be the fastest in degrading IBU indicating that BMM boosts the consortia performance, though no significant difference was observed (P-value>0.05). Comparing MBR2's bulk in SW and 3D printed gel, the latter seemed to be slower in degrading IBU. Although, the error bars at 110 h and the statistical analysis (P-value>0.05) indicate no clear difference between the bulk and the 3D printed gel.

To sum up, MBR2 (164 h) seemed to degrade IBU faster than MBR5 (339 h), when comparing the experiments duration of both consortia inside a 3D printed gel. However, considering the degradation of the nin gel for the later experiment, the degradation potential of the native SW microorganisms could have biased these findings.

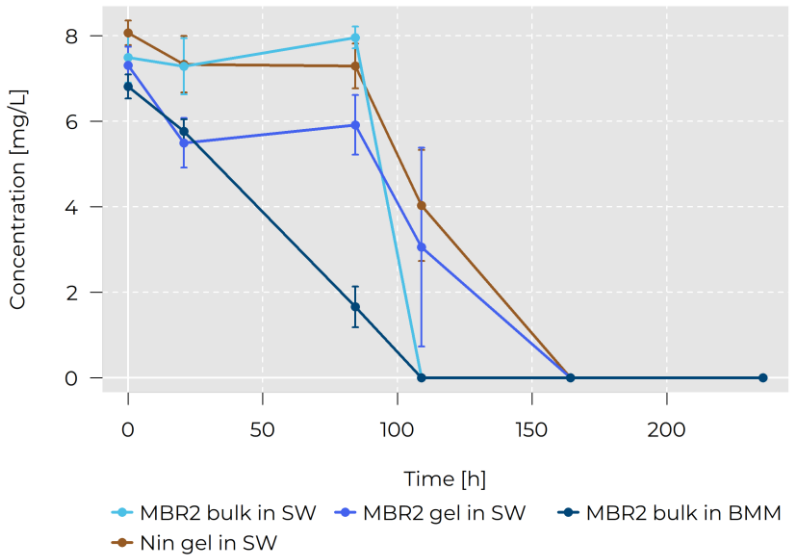

Figure 6 | IBU degradation experiment by MBR2 consortium represented as the change of IBU's concentration over time. Experiment carried out with MBR2 inoculated inside a 3D printed gel (**blue**) in SW and corresponding controls, inoculation of MBR2 from a liquid culture to SW (**light blue**), and to a rich medium, denoted as BMM (**dark blue**). In **brown** is represented the nin gel in SW. Values plotted are means ± standard deviations for three independent cultures.

4.1.2 Growth curve

For each degradation experiment a new culture was required, and its growth was measured in order to assess the fitness of the culture. In Figure 7 there is a representative growth curve in rich medium with 50 mg/L of IBU for both consortia in suspension. However, with the data points measured, it's hard to assess the growth kinetics of such consortia with accuracy. Despite this, it was still possible to observe that these consortia normally have a total OD_{600} increase of around 7x in a period as short as 20 h, after which the consortia plateaued. Also, these consortia had a relatively short lag phase, possibly because the bacteria harvested for the cryostocks were grown in comparable conditions as the new cultures, thereby minimizing the adaptation requirements. Both consortia had no significant difference in their growth (P-value>0.05).

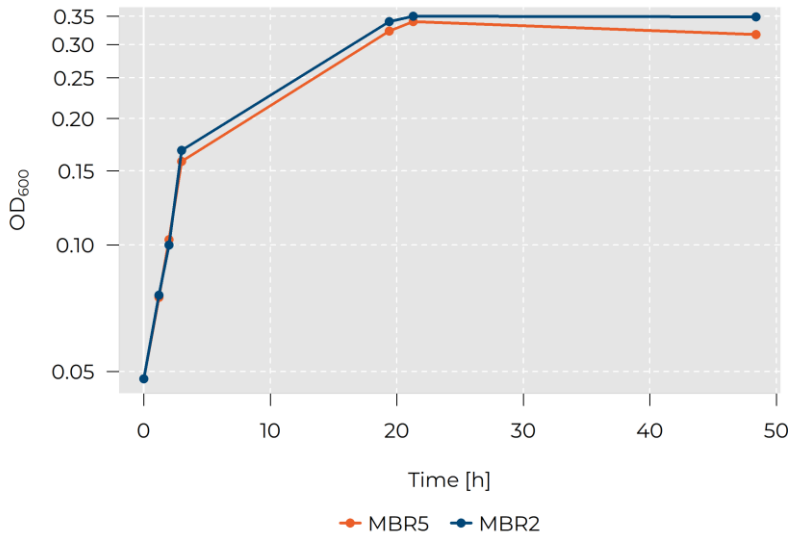

Figure 7 | Growth curve of MBR2 (**blue**) and MBR5 (**orange**) in a rich medium represented by the change of OD_{600} over time.

4.1.3 Survival test

After one week had elapsed the viability of MBR5 consortium was tested, shown in Figure 8. As can be observed, the consortium was able to grow in all tested conditions. In the case of MBR5 in a 3D printed gel that was expected, indicating that the consortium was still active. Regarding the bulk counterpart, a similar growth was expected, since both were inoculated in rich medium. In turn, the nin gel, which was not supposed to contain any kind of cells, also showed cell growth. These findings might be explained by the lack of sterile conditions during the process of preparing the ink and 3D printing, as the components of the bioink were not sterilized and the 3D printer itself wasn't in a sterile flow bench. Another possible scenario would be a contamination during the transfer of the gel or the finished 3D printed gels to the new culture. The fact that none of the conditions had significant differences (P-value>0.05) also suggests that the cell growth observed might not be caused solely by the inoculated consortium.

After two weeks of incubation in the degradation experiment, another survival assay was performed. This time not only the growth was measured to conclude about the consortia's viability but also the IBU's concentration to observe if the consortia still maintained the ability to degrade IBU while being inside the 3D printed gel. In Figure 9 the results of cell growth are shown. As previously demonstrated, cell growth was observed again in all tested conditions, therefore the consortium was able to survive for at least two weeks by degrading IBU inside the 3D printed gels. Indeed, no significant differences were detected between all conditions tested (P-value>0.05).

In terms of the actual IBU degradation, the MBR5 in a 3D printed gel maintained the capability of degrading IBU. The IBU removal rate was observed to remove more than 80% of IBU in a reasonable time (~72 h), compared to the previous degradation that took around 110 h for complete IBU removal. Finally, no signs of IBU degradation were observed for the nin gel, supporting the explanation that the cells observed to grow in Figure 9 were associated to a contamination and not the consortium that was misplaced in this control.

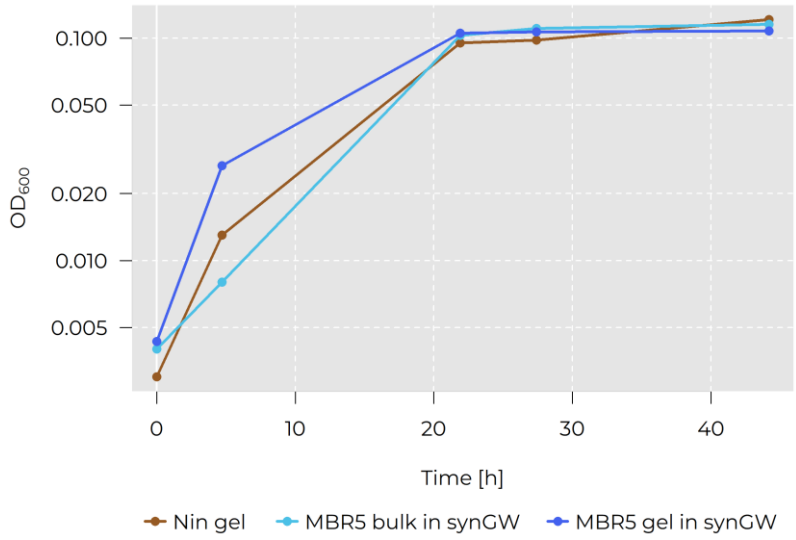

Figure 8 | Cell growth from the 3D printed gel or culture solution of different conditions from the degradation experiment represented by the change of OD_{600} over time. For the nin gel (**brown**) and MBR5 in gel (**blue**) a tiny piece of gel was evaluated, whilst for the MBR5 in bulk (**light blue**) a sample of the culture was used.

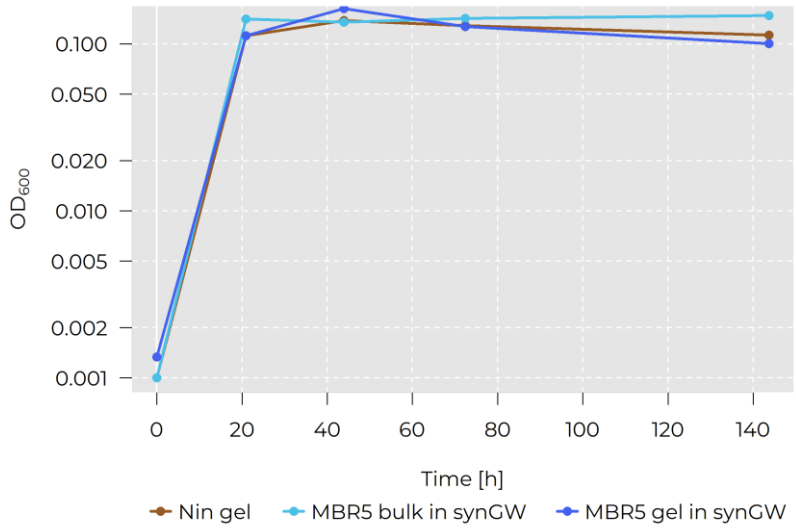

Figure 9 | Cell growth from the 3D printed gel or culture solution of different conditions from the degradation experiment represented by the change of OD_{600} over time. For the nin gel (**brown**) and MBR5 in gel (**blue**) a tiny piece of 3D printed gel was evaluated, whilst for the MBR5 in bulk (**light blue**) a volume of culture solution was used.

4.1.4 Ink toxicity test

From the previous degradation results, the IBU degradation by the consortia was less efficient when inside the 3D printed gels compared to the bulk conditions. This outcome raised the question whether the components of the ink were negatively affecting the performance or the survivability of the consortia. Figure 10 shows the results of the consortia's survivability while in the presence of said ink components. A generalized cell growth in all conditions was observed and both MBR2 and MBR5 had very similar growth patterns, as well as close OD_{600} values during the experiment, except in the Cells in BMM control and Cells in CMC, where MBR2 showed significant higher OD_{600} values (P-value<0.05) than MBR5, indicating that this consortium might have higher growth rates compared to MBR5. From the controls of this experiment, in both consortia the abiotic control shows no signs of growth (P-value<0.05), as expected. In the Cells in BMM control, which was expected to provide the best conditions for cell growth, the consortia grew equally or less than the samples with the bioink components. The bioink components seemed to have a positive or no influence on the consortia's growth, instead of harming them, as would have been expected. Among the ink components, MA-SA (P-value<0.05) appeared to benefit the cell growth the most, followed by ι-CA (P-value<0.05), whereas CMC (P-value>0.05) did not show a significant effect on the cell growth of both consortia. In the presence of the CL, the MBR2 consortium did not show significant higher cell growth (P-value>0.05), while for MBR5 it did (P-value<0.05), being the latter component as beneficial to MBR5's cell growth as ι-CA (P-value>0.05).

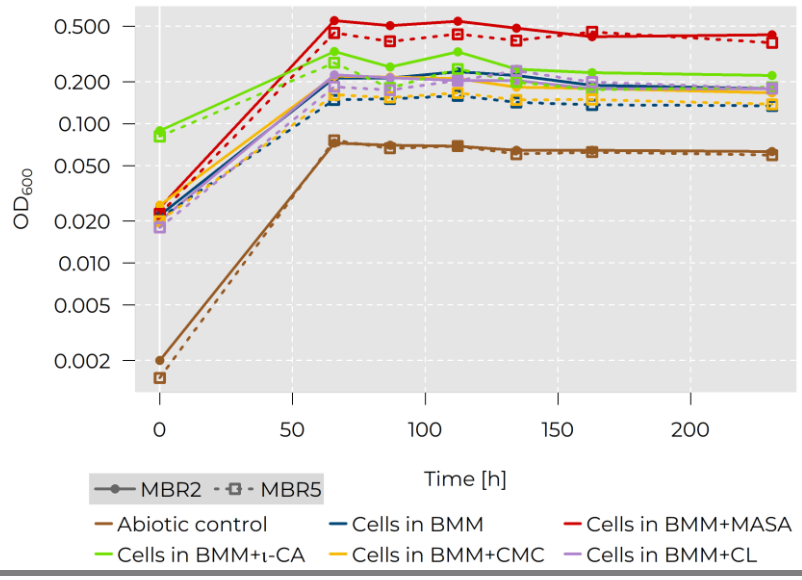

Figure 10 | Cell growth in the presence of the ink components represented by the change of OD_{600} over time. Each component is associated to a different color as follows **red** was assigned to MA-SA, **green** to ι-CA, **yellow** to CMC, **purple** to the CL, **brown** to the abiotic control, lacking cells and ink components, and **dark blue** to the positive control, lacking the ink components. MBR2 data is represented with solid lines with dots, while MBR5 data is represented with dashed lines with hole squares.

The IBU degradation of the samples in the ink toxicity assay is illustrated in Figure 11. MBR2 consortium was able to degrade IBU below detectable levels in an unexpectedly short time (<65 h) compared to previous results (Figure 6). With MBR5 the results were comparable, even though the degradation was slower than MBR2. Particularly interesting was the decreased IBU degradation rate of MBR5 in the presence of MA-SA compared to other conditions, reinforcing the hypothesis that this consortium might be using other carbon sources before IBU, thus consequently decreasing its degradation. Furthermore, this finding suggested that this consortium might also be degrading the ink itself, which was corroborated by visual evaluation of the 3D printed gel fragmentation (appendix 7.2). As expected, the abiotic controls demonstrated no IBU degradation.

To sum up, the components did not seem to have any harmful effect to the bacterial consortia, however, a slight decrease in IBU degradation rate was observed for MBR5 while in the presence of MA-SA.

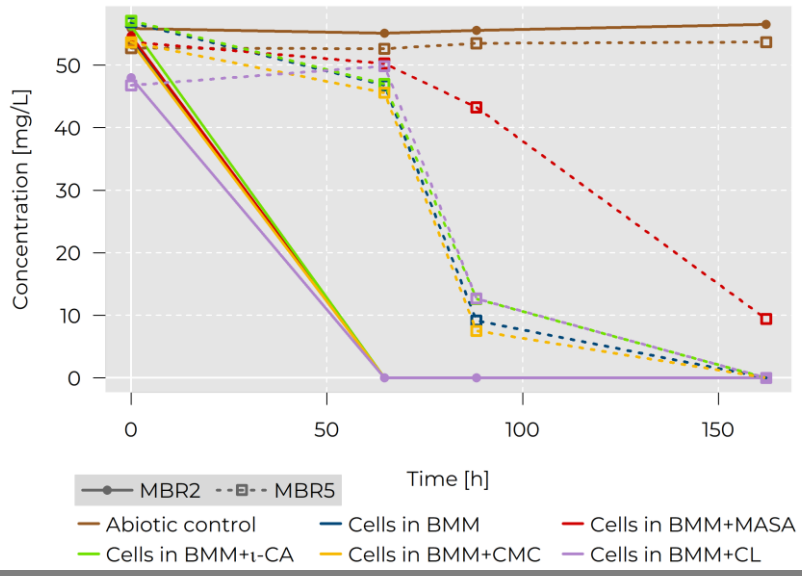

Figure 11 | IBU degradation in the presence of the ink components represented by the change of IBU's concentration over time. Each component is associated to a different color as follows **red** was assigned to MA-SA, **green** to ι-CA, **yellow** to CMC, **purple** to the CL, **brown** to the abiotic control, lacking cells and ink components, and **dark blue** to the positive control, lacking the ink components. MBR2 data is represented with solid lines with dots, while MBR5 data is represented with dashed lines with hole squares.

4.2 Plate isolation

After establishing that the MBR2 consortium seemed to have higher degradation rates compared to MBR5, the next experiments aimed to isolate single strains from MBR2 capable of degrading IBU without the support of their native consortium. This task would as a first step simplify the experiment by working only with single strains instead of complex and unknown communities. The isolation procedure yielded 9 different isolates, 8 of which were further assessed for their capability in degrading IBU, as well as their growth.

Figure 12 depicts the IBU degradation performance of the isolated strains in rich medium. The isolate no. 3 (MBRi3), shown in yellow, performed at unexpectedly high degradation rates, corroborated by the significant difference compared to all the remaining isolates (P-value<0.05). After around 80 h this isolate was capable of degrading IBU to levels below the limit of quantification of the HPLC, 3 mg/L, comparable to the time MBR2 required to degrade IBU in previous experiments. Unlike MBRi3, all other isolates showed degradation of IBU for a much longer incubation time. Nevertheless, isolates no. 4 and 7 showed clear signs of IBU degradation after almost 700 h, whilst no. 2, 6 and 9 might be additional possible single strain degraders with a much slower degradation. Isolates no. 1 and 5 did not show any capacity to degrade IBU. However, no significant difference was observed between isolate 2 and 9 (P-value>0.05).

Figure 13 shows the population growth of the different isolated strains over time in rich medium. Most of the isolates showed significant differences in their growth (P-value<0.05), apart from isolate 3 and 4 (P-value>0.05). In general, most strains seemed to have a relatively small increase in OD_{600}, compared to MBR2's OD_{600} increase observed previously.

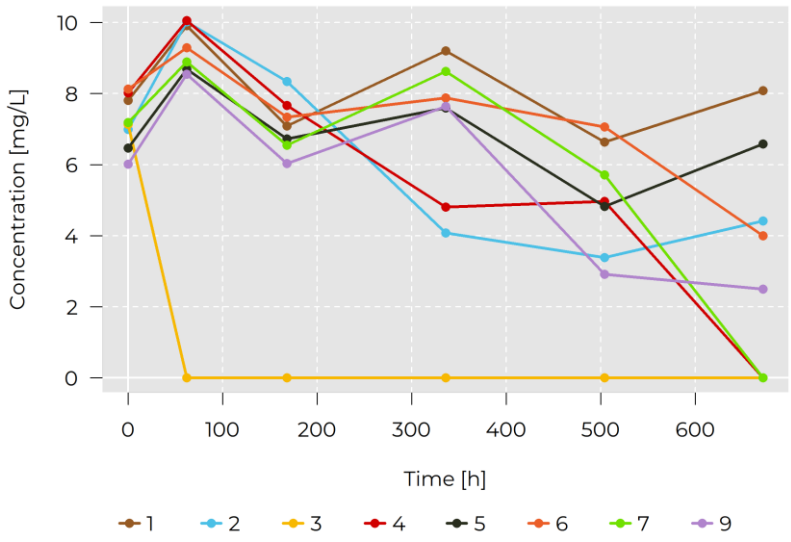

Figure 12 | IBU degradation by MBR2 isolated strains in rich medium at 25 °C represented by the change of IBU's concentration over time. Each strain is associated to a different number and color.

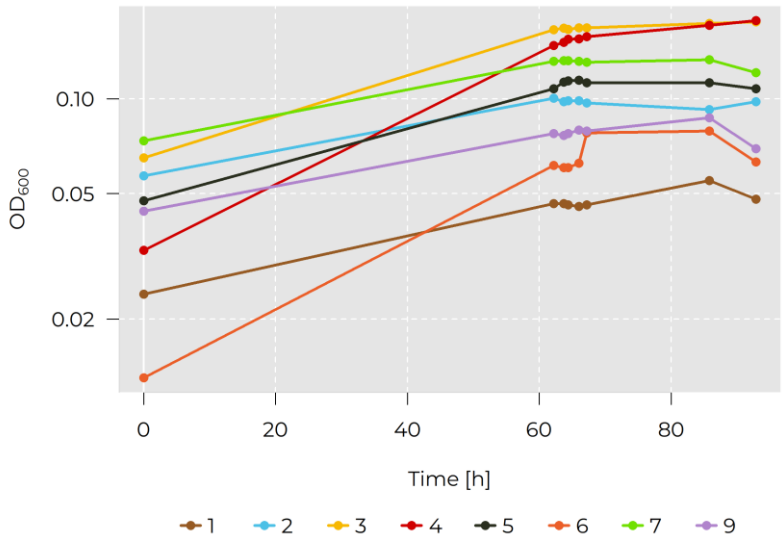

Figure 13 | Cell growth from the MBR2 isolated strains in rich medium at 25 °C represented by the change of OD_{600} over time. Each strain is associated to a different number and color.

4.3 Dilution "isolation"

Figure 14 shows the IBU degradation performance of the different diluted samples. As mentioned previously, four serial dilutions of MBR2 consortium were performed. As the dilution steps 10^{-3} and 10^{-4} showed the same behavior, the datapoints for dilution 10^{-3} were completely covered by the data points for the line of dilution 10^{-4}, supported as well by the statistical analysis (P-value>0.05).This suggests that dilution 10^{-3} and 10^{-4} had virtually the same communities, furthermore, suggesting that all dilution steps until 10^{-4} exhibited a comparable community to the non-diluted consortium. The higher IBU concentration for dilution 10^{-5} was probably due to pipetting errors. The sample of dilution 10^{-5} featured different behavior compared to the less diluted samples (P-value<0.05), which for

dilution 10^{-6} is less clear (P-value>0.05). In fact, by increasing dilution factors depletion of IBU by microorganisms should take longer, a possible consequence of diminishing microbial diversity through dilution, leading to a possible disruption of IBU co-metabolism. Another consequence of diluting is the decrease of loaded biomass, which translates to lower degradation rates at the beginning for high diluted cultures. Interestingly dilution 10^{-6} degraded IBU faster than dilution 10^{-5} (P-value<0.05), indicating this might be a promising dilution sample to be used in further experiments in a 3D printed gel. Despite these results, a further experiment showing a dilution where no IBU is degrading would be required in order to assess the highest degrading dilution step.

The growth curves of the diluted MBR2 cultures are displayed in Figure 15. Remarkably, dilution 10^{-5} grew faster compared to the other dilutions (P-value<0.05) and performed slower degradation of IBU (Figure 14). A possible explanation for this behavior would be that this specific dilution sample appeared to start with a higher IBU concentration, which would suggest a higher carbon availability and therefore higher biomass yield potential. The remaining dilutions also showed significant differences in growth (P-value<0.05), except for dilution 10^{-4} and 10^{-6}, which datapoints appear to almost completely overlap (P-value>0.05).

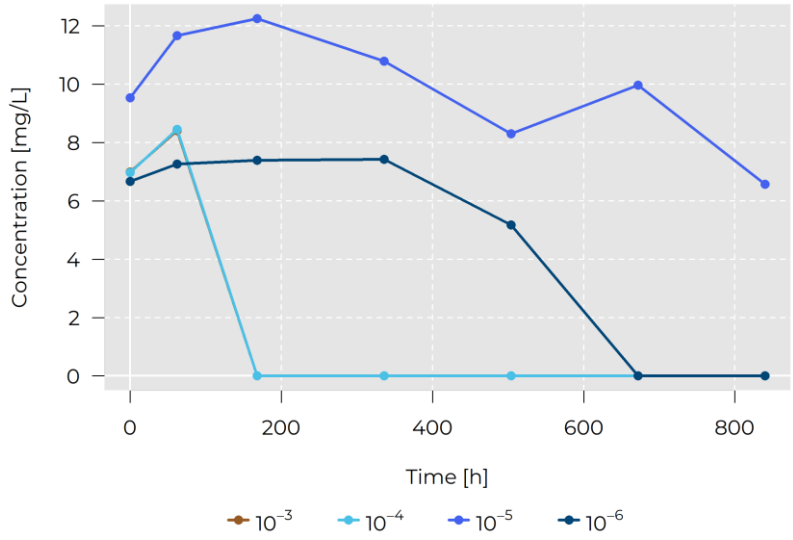

Figure 14 | IBU degradation in rich medium liquid cultures inoculated with MBR2 serial dilutions represented by the change of IBU's concentration over time. Each dilution of the original consortium is associated to a different name and color.

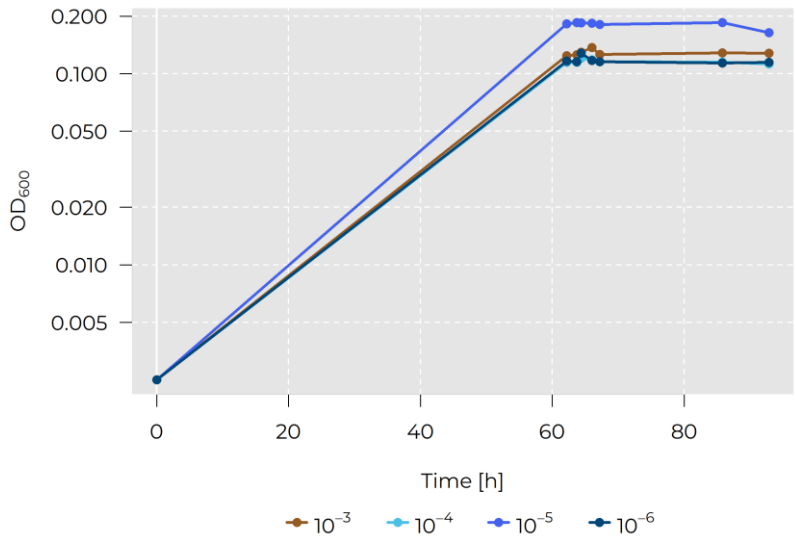

Figure 15 | Cell growth from the MBR2 serial dilutions from liquid cultures represented by the change of OD_{600} over time. Each dilution is associated to a different name and color.

To further investigate the composition of the diluted MBR2, a community 16S rRNA gene-based analysis was conducted for cultures of 10^{-5} and 10^{-6} dilution factors. In Figure 16 is displayed the composition of the communities to the family level. Both diluted cultures contained a broad variety of bacteria belonging to six different families, mostly from *Comamonadaceae* and *Enterobacteriaceae* representing around 35% and 40% of the total abundance, respectively, indicating that the dilution factors employed were not high enough to obtain individual strains. In fact, both samples shared a very similar community, suggesting that a higher dilution factor step, for example, 50x instead of 10x, could be used to obtain more refined cultures. On the other hand, samples 10^{-5} and 10^{-6} exhibited different IBU degradation behaviors, despite the similarity between communities suggested by the results.

In summary, a different community was obtained by dilution of MBR2 as observed by the distinct degradation behaviors, even though this method did not result with isolated strains.

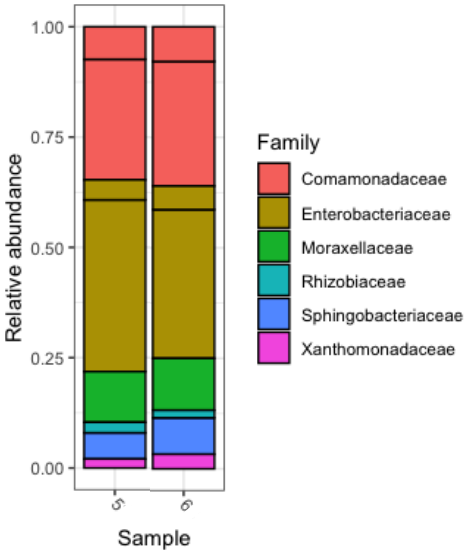

Figure 16 | Composition of the 10^{-5} and 10^{-6} diluted MBR2 consortium represented by sample 5 and 6, respectively, to the level of family.

4.4 Isolate 3

From the two isolation methods carried out and the isolates obtained, isolate MBRi3 from the plate isolation was chosen to be used for further experiments, due to its high IBU degradation potential.

4.4.1 Degradation experiment

Like MBR2 and MBR5 consortia, MBRi3's degradation was tested inside a 3D printed gel in SW and the results obtained are shown in Figure 17. MBRi3 in rich medium degraded IBU considerably fast, possibly in a less than around 60 h. Once again, MBRi3 in a 3D printed gel seems to perform slightly worse than its bulk in poor medium counterpart, which may indicate that the 3D printed gel might be affecting the strain performance. Despite this, the strain inside the 3D printed gel was still capable of degrading IBU below quantification in 115 h while still inside an integral 3D printed gel, before it started fragmenting. Therefore, no major change in the conditions occurred during the experiment. In turn, the empty 3D printed gel behaved similar to MBR2's degradation experiment, most probably because it suffers from the same non-sterility issue, which appears to jeopardize the validity of this control. However, no significant difference was observed between any of the conditions tested and the control (P value > 0.05).

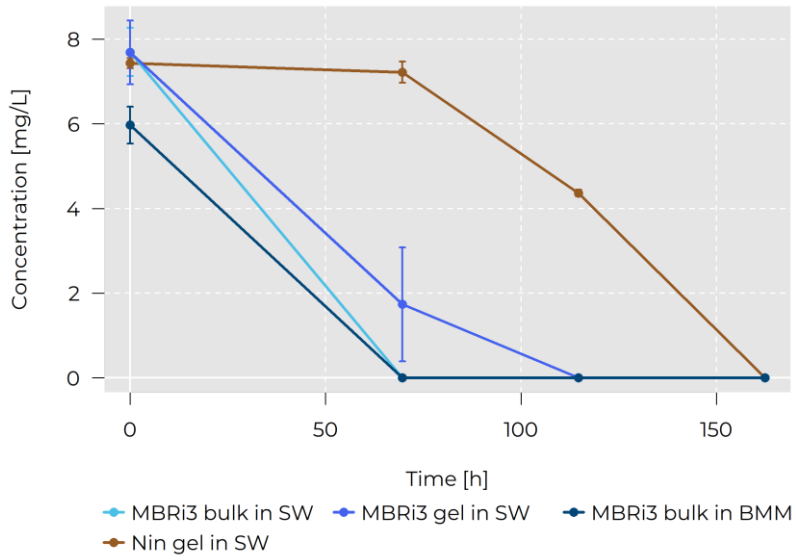

Figure 17 | IBU degradation experiment by MBRi3 strain represented by the change of IBU's concentration over time. Experiment carried out with MBRi3 inoculated inside a 3D printed gel (**blue**) in SW and corresponding controls, inoculation of MBRi3 from a liquid culture to SW (**light blue**), and to a rich medium, denoted as BMM (**dark blue**). In **brown** is represented the empty 3D printed gel in SW. Values plotted are means ± standard deviations for three independent cultures.

4.4.2 Growth curve

Recalling Figure 13 and comparing to Figure 18, MBRi3's growth curves are identical, but the latter adds some more time points allowing to confirm that this isolate had an OD_{600} increase of ca. 4x during a period of ca. 40 h. Compared to MBR2's growth curve is possible to say that this isolate had a slow growth and probably contributes less to the OD_{600} increase observed in Figure 7.

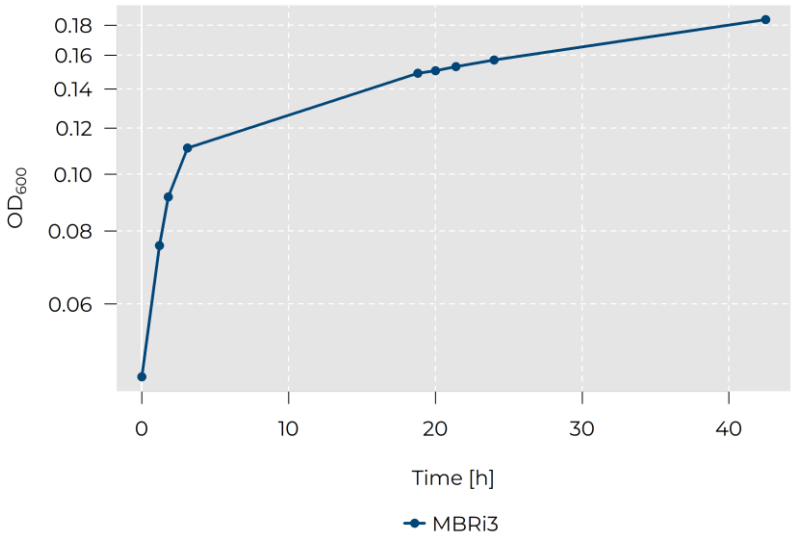

Figure 18 | Growth curve of MBRi3 in rich medium at 25 °C represented by the change of OD_{600} over time.

5 Conclusion

The main goal of this thesis consisted in developing a bioremediation method by means of producing a gel through 3D printing technology incorporating microorganisms capable of degrading IBU in GW-like conditions. This was successfully achieved by 3D printing of an alginate-based hydrogel with two bacterial consortia and a single strain. The strain was isolated from a colony of the consortium with faster degradation potential (MBR2).

All the 3D printed samples showed reasonable times necessary to degrade IBU, the consortia MBR2 and MBR5 took around 164 h and 339 h, respectively. While the single strain, MBRi3, achieved this within 115 h. However, the MBR5 consortium was cultured in synGW medium, whilst for MBR2 and MBRi3 non-sterile SW sampled from a water body was used. Therefore, the significant increase of degradation rates in the latter condition was likely influenced by the presence of other microorganisms in the SW. Moreover, the hydrogel in this medium often started to fragment after about a week, another possible consequence of the presence of external microorganisms capable of feeding on the polymer components.

The survivability of the consortia and possible negative effects of the employed hydrogel were assessed, since some of the components are described to be cytotoxic. The consortia from a portion of the hydrogels were able to grow in a new medium indicating that the consortia were still active and degrading IBU. This also allowed to verify that the 3D printed gel can maintain the consortia alive for at least two weeks. In turn, no adverse effects were observed regarding the cell growth and IBU degradation. In fact, some components, such as MA-SA and ι-CA, seemed to promote cell growth. Conversely, MA-SA showed to slow down the degradation of IBU for MBR5, suggesting this component was used as an additional carbon source along with IBU.

A 16S rRNA gene sequence community analysis was performed on diluted MBR2 cultures. Despite, no reduction in complexity was achieved with the applied dilution factors, it was verified that MBR2 is a complex consortium of bacteria belonging to six different families, mostly from the *Comamonadaceae* and *Enterobacteriaceae* representing around 35% and 40% of the total abundance, respectively.

5.1 Future work and limitations

The results of the present work opened new opportunities for further experiments and allowed to point out aspects that need further improvement. For instance, the plate isolation assay yielded several different single strains. As a next step a DNA analysis of the most promising single strain degraders would provide more information about the microorganisms' identity, as well as insights of their roles on IBU degradation. By further assessing the degradation potential of several different strains, the 3D printing could provide an optimal approach for a spatially defined artificial biofilm. By employing several different strains in different layers, enabling them to perform each one a fraction of the metabolic pathway of IBU as efficiently as possible.

A major challenge was the fragmentation of the 3D printed gel during the experiments, assumed to be caused by the native microorganisms present in the SW, therefore, suggesting the need to

increase the gel's durability. This could be performed by increasing the crosslinking degree or changing the main polymer to a less biodegradable one.

To take this project a level further the replication of more accurate environmental conditions could be employed. It is well-known that the environment is not contaminated with a sole compound but by a complex mixture of different pollutants. Besides IBU other environmentally relevant pharmaceuticals could be jointly assessed. Furthermore, 3D printed gels incorporating distinct layers of microorganisms capable of degrading different compounds could be employed in a broader degradation experiment targeting multiple pollutants.

Moreover, the applied concentrations in the previous experiment (5-50 mg/L) did not correspond to environmental values in water bodies of <1 mg/L. Such low levels cannot be detected by the applied analytical method and would require more complex equipment. Despite their complexity and cost, equipment, including LC-MS/MS, could more accurately analyze IBU's concentration, while at the same time measuring other byproducts of IBU to ensure total mineralization.

6 References

[1] Z. Stevanović, "Karst waters in potable water supply: a global scale overview," *Environ Earth Sci*, 78, 662, 2019, doi: 10.1007/s12665-019-8670-9.

[2] D. J. Lapworth, T. B. Boving, D. K. Kreamer, S. Kebede, and P. L. Smedley, "Groundwater quality: Global threats, opportunities and realising the potential of groundwater," *Sci of the Total Environ*, 811, 152471, 2022, doi: 10.1016/j.scitotenv.2021.152471.

[3] N. M. Burri, R. Weatherl, C. Moeck, and M. Schirmer, "A review of threats to groundwater quality in the anthropocene," *Sci of the Total Environ,* 684, 2019, doi: 10.1016/j.scitotenv.2019.05.236.

[4] R. Silori *et al.*, "Global groundwater vulnerability for Pharmaceutical and Personal care products (PPCPs): The scenario of second decade of 21st century," *J Environ Manage*, 320, 115703, 2022, doi: 10.1016/j.jenvman.2022.115703.

[5] C. Grady, S. Weng, and E. Blatchley III, "Global Potable Water: Current Status, Critical Problems, and Future Perspectives," in *Handbook of Environ Chem*, 2014, doi: 10.1007/978-3-319-06563-2_2.

[6] K. W. F. Howard, "Sustainable cities and the groundwater governance challenge," *Environ Earth Sci*, 73, 2015, doi: 10.1007/s12665-014-3370-y.

[7] B. C. Pires, T. A. do Nascimento, F. V. A. Dutra, and K. B. Borges, "Removal of a non-steroidal anti-inflammatory by adsorption on polypyrrole/multiwalled carbon nanotube composite—Study of kinetics and equilibrium in aqueous medium," *Colloids Surf A Physicochem Eng Asp*, 578, 2019, doi: 10.1016/j.colsurfa.2019.123583.

[8] Y. Fan, H. Li, and G. Miguez-Macho, "Global patterns of groundwater table depth," *Sci* , 339, 6122, 2013, doi: 10.1126/science.1229881.

[9] A. Jurado, E. Vázquez-Suñé, and E. Pujades, "Urban groundwater contamination by non-steroidal anti-inflammatory drugs," *Water* , 13, 5, 2021, doi: 10.3390/w13050720.

[10] E. N. Evgenidou, I. K. Konstantinou, and D. A. Lambropoulou, "Occurrence and removal of transformation products of PPCPs and illicit drugs in wastewaters: A review," *Sci of the Total Environ*, 505, 2015, doi: 10.1016/j.scitotenv.2014.10.021.

[11] L. M. Gómez-Oliván, M. Galar-Martínez, S. García-Medina, A. Valdés-Alanís, H. Islas-Flores, and N. Neri-Cruz, "Genotoxic response and oxidative stress induced by

diclofenac, ibuprofen and naproxen in Daphnia magna," *Drug Chem Toxicol*, 37, 4, 2014, doi: 10.3109/01480545.2013.870191.

[12] F. T. Mathias *et al.*, "Effects of low concentrations of ibuprofen on freshwater fish Rhamdia quelen," *Environ Toxicol Pharmacol*, 59, 2018, doi: 10.1016/j.etap.2018.03.008.

[13] V. Iori, F. Pietrini, and M. Zacchini, "Assessment of ibuprofen tolerance and removal capability in Populus nigra L. by in vitro culture," *J Hazard Mater*, 229–230, 2012, doi: 10.1016/j.jhazmat.2012.05.097.

[14] B. Tiwari, B. Sellamuthu, Y. Ouarda, P. Drogui, R. D. Tyagi, and G. Buelna, "Review on fate and mechanism of removal of pharmaceutical pollutants from wastewater using biological approach," *Bioresour Technol*, 224, 2017, doi: 10.1016/j.biortech.2016.11.042.

[15] M. Patel, R. Kumar, K. Kishor, T. Mlsna, C. U. Pittman, and D. Mohan, "Pharmaceuticals of emerging concern in aquatic systems: Chemistry, occurrence, effects, and removal methods," *Chem Rev*, 119, 6, 2019, doi: 10.1021/acs.chemrev.8b00299.

[16] C. Escapa, R. N. Coimbra, S. Paniagua, A. I. García, and M. Otero, "Paracetamol and salicylic acid removal from contaminated water by microalgae," *J Environ Manage*, 203, 2017, doi: 10.1016/j.jenvman.2016.06.051.

[17] J. Radjenović, M. Petrović, and D. Barceló, "Fate and distribution of pharmaceuticals in wastewater and sewage sludge of the conventional activated sludge (CAS) and advanced membrane bioreactor (MBR) treatment," *Water Res*, 43, 3, 2009, doi: 10.1016/j.watres.2008.11.043.

[18] H. Islas-Flores and L. M. Gómez-Oliván, "Legislation Controlling the Discharge of Pharmaceuticals into the Environment," in *Ecopharmacovigilance: Multidisciplinary Approaches to Environ Saf of Medicines*,2019. doi: 10.1007/698_2017_170.

[19] R. B. de A. Aragão, D. Semensatto, L. A. Calixto, and G. Labuto, "Pharmaceutical market, environmental public policies and water quality: the case of the São Paulo Metropolitan Region, Brazil," *Cad Saude Publica*, 36, 2020, doi: 10.1590/0102-311X00192319.

[20] M. Parolini, A. Binelli, and A. Provini, "Chronic effects induced by ibuprofen on the freshwater bivalve Dreissena polymorpha," *Ecotoxicol Environ Saf*, 74, 6, 2011, doi: 10.1016/j.ecoenv.2011.04.025.

[21] A. Khadir, M. Motamedi, M. Negarestani, M. Sillanpää, and M. Sasani, "Preparation of a nano bio-composite based on cellulosic biomass and conducting polymeric nanoparticles for ibuprofen removal: Kinetics, isotherms, and energy site distribution," *Int J Biol Macromol*, 162, 2020, doi: 10.1016/j.ijbiomac.2020.06.095.

[22] M. Saravanan, K. U. Devi, A. Malarvizhi, and M. Ramesh, "Effects of Ibuprofen on hematological, biochemical and enzymological parameters of blood in an Indian major carp, Cirrhinus mrigala," *Environ Toxicol Pharmacol*, 34, 1, 2012, doi: 10.1016/j.etap.2012.02.005.

[23] C. Zwiener, S. Seeger, T. Glauner, and F. H. Frimmel, "Metabolites from the biodegradation of pharmaceutical residues of ibuprofen in biofilm reactors and batch experiments," *Anal Bioanal Chem*, 372, 4, 2002, doi: 10.1007/s00216-001-1210-x.

[24] G. L. Nielsen, H. T. Sørensen, H. Larsen, and L. Pedersen, "Risk of adverse birth outcome and miscarriage in pregnant users of non-steroidal anti-inflammatory drugs: Population based observational study and case-control study," *Br Med J*, 322, 7281, 2001, doi: 10.1136/bmj.322.7281.266.

[25] Natural Resource Management Ministerial Council, *Australian Guidelines For Water Recycling: Managing Health And Environmental Risks (Phase 2), Augmentation Of Drinking Water Supplies*. 2008.

[26] K. K. Barnes, D. W. Kolpin, E. T. Furlong, S. D. Zaugg, M. T. Meyer, and L. B. Barber, "A national reconnaissance of pharmaceuticals and other organic wastewater contaminants in the United States - I) Groundwater," *Sci of the Total Environ*, 402, 2–3, 2008, doi: 10.1016/j.scitotenv.2008.04.028.

[27] R. Loos *et al.*, "Pan-European survey on the occurrence of selected polar organic persistent pollutants in ground water," *Water Res*, 44, 14, 2010, doi: 10.1016/j.watres.2010.05.032.

[28] Th. Heberer, K. Schmidt-Bäumler, and H.-J. Stan, "Occurrence and Distribution of Organic Contaminants in the Aquatic System in Berlin. Part I: Drug Residues and other Polar Contaminants in Berlin Surface and Groundwater," *Acta hydrochim. hydrobiologica*, 26, 5, 1998.

[29] M. Rabiet, A. Togola, F. Brissaud, J. L. Seidel, H. Budzinski, and F. Elbaz-Poulichet, "Consequences of treated water recycling as regards pharmaceuticals and drugs in surface and ground waters of a medium-sized mediterranean catchment," *Environ Sci Technol*, 40, 17, 2006, doi: 10.1021/es060528p.

[30] C. Cruz-Morató *et al.*, "Degradation of pharmaceuticals in non-sterile urban wastewater by Trametes versicolor in a fluidized bed bioreactor," *Water Res*, 47, 14, 2013, doi: 10.1016/j.watres.2013.06.007.

[31] A. David and K. Pancharatna, "Developmental anomalies induced by a non-selective COX inhibitor (ibuprofen) in zebrafish (Danio rerio)," *Environ Toxicol Pharmacol*, 27, 3, 2009, doi: 10.1016/j.etap.2009.01.002.

[32] N. Vieno, T. Tuhkanen, and L. Kronberg, "Removal of pharmaceuticals in drinking water treatment: Effect of chemical coagulation," *Environ Technol*, 27, 2, 2006, doi: 10.1080/09593332708618632.

[33] K. Fischer, M. Grimm, J. Meyers, C. Dietrich, R. Gläser, and A. Schulze, "Photoactive microfiltration membranes via directed synthesis of TiO2 nanoparticles on the polymer surface for removal of drugs from water," *J Memb Sci*, 478, 2015, doi: 10.1016/j.memsci.2015.01.009.

[34] A. Khadir, M. Negarestani, and A. Mollahosseini, "Sequestration of a non-steroidal anti-inflammatory drug from aquatic media by lignocellulosic material (Luffa cylindrica) reinforced with polypyrrole: Study of parameters, kinetics, and equilibrium," *J Environ Chem Eng*, 8, 3, 2020, doi: 10.1016/j.jece.2020.103734.

[35] A. Dawas-Massalha, S. Gur-Reznik, S. Lerman, I. Sabbah, and C. G. Dosoretz, "Co-metabolic oxidation of pharmaceutical compounds by a nitrifying bacterial enrichment," *Bioresour Technol*, 167, 2014, doi: 10.1016/j.biortech.2014.06.003.

[36] E. Marco-Urrea, M. Pérez-Trujillo, T. Vicent, and G. Caminal, "Ability of white-rot fungi to remove selected pharmaceuticals and identification of degradation products of ibuprofen by Trametes versicolor," *Chemosphere*, 74, 6, 2009, doi: 10.1016/j.chemosphere.2008.10.040.

[37] A. I. Rodarte-Morales, G. Feijoo, M. T. Moreira, and J. M. Lema, "Operation of stirred tank reactors (STRs) and fixed-bed reactors (FBRs) with free and immobilized Phanerochaete chrysosporium for the continuous removal of pharmaceutical compounds," *Biochem Eng J*, 66, 2012, doi: 10.1016/j.bej.2012.04.011.

[38] V. Matamoros, C. Arias, H. Brix, and J. M. Bayona, "Removal of Pharmaceuticals and Personal Care Products (PPCPs) from Urban Wastewater in a Pilot Vertical Flow Constructed Wetland and a Sand Filter," *Environ Sci Technol*, 41, 23, 2007, doi: 10.1021/es071594.

[39] A. Arca-Ramos, V. V. Kumar, G. Eibes, M. T. Moreira, and H. Cabana, "Recyclable cross-linked laccase aggregates coupled to magnetic silica microbeads for elimination of pharmaceuticals from municipal wastewater," *Environ Sci and Pollution Res*, 23, 9, 2016, doi: 10.1007/s11356-016-6139-x.

[40] B. I. Escher, W. Pronk, M. J. F. Suter, and M. Maurer, "Monitoring the removal efficiency of pharmaceuticals and hormones in different treatment processes of source-separated urine with bioassays," *Environ Sci Technol*, 40, 16, 2006, doi: 10.1021/es060598w.

[41] A. Nzila, "Update on the cometabolism of organic pollutants by bacteria," *Environ Pollution*, 178, 2013, doi: https://doi.org/10.1016/j.envpol.2013.03.042.

[42] J. B. Quintana, S. Weiss, and T. Reemtsma, "Pathways and metabolites of microbial degradation of selected acidic pharmaceutical and their occurrence in municipal wastewater treated by a membrane bioreactor," *Water Res*, 39, 12, 2005, doi: 10.1016/j.watres.2005.04.068.

[43] I. A. Vasiliadou *et al.*, "Biological removal of pharmaceutical compounds using white-rot fungi with concomitant FAME production of the residual biomass," *J Environ Manage*, 180, 2016, doi: 10.1016/j.jenvman.2016.05.035.

[44] R. Pishgar, G. Najafpour, B. N. Neya, N. Mousavi, and Z. Bakhshi, "Anaerobic Biodegradation of Phenol: Comparative Study of Free and Immobilized Growth," *Iranica J of Energy & Environ*, 2, 4, 2011, doi: 10.5829/idosi.ijee.2011.02.04.2361.

[45] A. Ruiz-Marin, L. G. Mendoza-Espinosa, and T. Stephenson, "Growth and nutrient removal in free and immobilized green algae in batch and semi-continuous cultures treating real wastewater," *Bioresour Technol*, 101, 1, 2010, doi: 10.1016/j.biortech.2009.02.076.

[46] M. G. Ziagova, A. I. Koukkou, and M. Liakopoulou-Kyriakides, "Optimization of cultural conditions of Arthrobacter sp. Sphe3 for growth-associated chromate(VI) reduction in free and immobilized cell systems," *Chemosphere*, 95, 2014, doi: 10.1016/j.chemosphere.2013.09.112.

[47] Y. J. Seol, H. W. Kang, S. J. Lee, A. Atala, and J. J. Yoo, "Bioprinting technology and its applications," *European J of Cardio-thoracic Surgery*, 46, 3, 2014, doi: 10.1093/ejcts/ezu148.

[48] M. Hasany *et al.*, "Synthesis, properties, and biomedical applications of alginate methacrylate (ALMA)-based hydrogels: Current advances and challenges," *Appl Mater Today*, 24, 2021, doi: 10.1016/j.apmt.2021.101150.

[49] I. Noshadi *et al.*, "In vitro and in vivo analysis of visible light crosslinkable gelatin methacryloyl (GelMA) hydrogels," *Biomater Sci*, 5, 10, 2017, doi: 10.1039/c7bm00110j.

[50] T. Xu *et al.*, "Viability and electrophysiology of neural cell structures generated by the inkjet printing method," *Biomater*, 27, 19, 2006, doi: 10.1016/j.biomaterials.2006.01.048.

[51] L. Shengjie, Z. Xiong, X. Wang, Y. Yan, H. Liu, and R. Zhang, "Direct fabrication of a hybrid cell/hydrogel construct by a double-nozzle assembling technology," *J Bioact Compat Polym*, 24, 3, 2009, doi: 10.1177/0883911509104094.

[52] P. Rider, Ž. P. Kačarević, S. Alkildani, S. Retnasingh, and M. Barbeck, "Bioprinting of tissue engineering scaffolds," *J Tissue Eng*, 9, 2018, doi: 10.1177/2041731418802090.

[53] S. Kyle, Z. M. Jessop, A. Al-Sabah, and I. S. Whitaker, "'Printability'' of Candidate Biomaterials for Extrusion Based 3D Printing: State-of-the-Art,'" *Adv Healthc Mater*, 6, 16, 2017, doi: 10.1002/adhm.201700264.

[54] B. Duan, L. A. Hockaday, K. H. Kang, and J. T. Butcher, "3D Bioprinting of heterogeneous aortic valve conduits with alginate/gelatin hydrogels," *J Biomed Mater Res A*, 101 A, 5, 2013, doi: 10.1002/jbm.a.34420.

[55] I. Apsite, J. M. Uribe, A. F. Posada, S. Rosenfeldt, S. Salehi, and L. Ionov, "4D biofabrication of skeletal muscle microtissues," *Biofabrication*, 12, 1, 2020, doi: 10.1088/1758-5090/ab4cc4.

[56] B. Stubbe, A. Mignon, H. Declercq, S. Van Vlierberghe, and P. Dubruel, "Development of Gelatin-Alginate Hydrogels for Burn Wound Treatment," *Macromol Biosci*, 19, 8, 2019, doi: 10.1002/mabi.201900123.

[57] L. Chen, S. M. Kenkel, P. H. Hsieh, M. C. Gryka, and R. Bhargava, "Freeform Three-Dimensionally Printed Microchannels via Surface-Initiated Photopolymerization Combined with Sacrificial Molding," *ACS Appl Mater Interfaces*, 12, 44, 2020, doi: 10.1021/acsami.0c12158.

[58] S. H. Moon, H. J. Hwang, H. R. Jeon, S. J. Park, I. S. Bae, and Y. J. Yang, "Photocrosslinkable natural polymers in tissue engineering," *Front Bioeng Biotechnol*, 11, 2023, doi: 10.3389/fbioe.2023.1127757.

[59] R. Popielarz and O. Vogt, "Effect of coinitiator type on initiation efficiency of two-component photoinitiator systems based on eosin," *J Polym Sci A Polym Chem*, 46, 11, 2008, doi: 10.1002/pola.22688.

[60] *Test No. 303: Simulation Test - Aerobic Sewage Treatment -- A: Activated Sludge Units; B: Biofilms*. in OECD Guidelines for the Testing of Chemicals, Section 3. OECD, 2001. doi: 10.1787/9789264070424-en.

7 Appendix

7.1 Mineral medium Brunner recipe

Microorganisms DSMZ

457. MINERAL MEDIUM (BRUNNER)

Na_2HPO_4	2.44	g
KH_2PO_4	1.52	g
$(NH_4)_2SO_4$	0.50	g
$MgSO_4$ x 7 H_2O	0.20	g
$CaCl_2$ x 2 H_2O	0.05	g
Trace element solution SL-4 (see below)	10.00	ml
Distilled water	1000.00	ml

Adjust pH to 6.9.
Prepare a separate solution of the phosphates and autoclave separately. Combine the two solutions after cooling.

Rehydrate and cultivate lyophilized cells in complex medium (e.g. medium 1, 220 or 535). After this reactivation, cultivate in mineral medium 457 with the appropriate carbon source.

Trace element solution SL-4:

EDTA	0.50	g
$FeSO_4$ x 7 H_2O	0.20	g
Trace element solution SL-6 (see below)	100.00	ml
Distilled water	900.00	ml

Trace element solution SL-6:

$ZnSO_4$ x 7 H_2O	0.10	g
$MnCl_2$ x 4 H_2O	0.03	g
H_3BO_3	0.30	g
$CoCl_2$ x 6 H_2O	0.20	g
$CuCl_2$ x 2 H_2O	0.01	g
$NiCl_2$ x 6 H_2O	0.02	g
Na_2MoO_4 x 2 H_2O	0.03	g
Distilled water	1000.00	ml

7.2 Gel fragmentation – isolate 3 degradation experiment

- Day 0

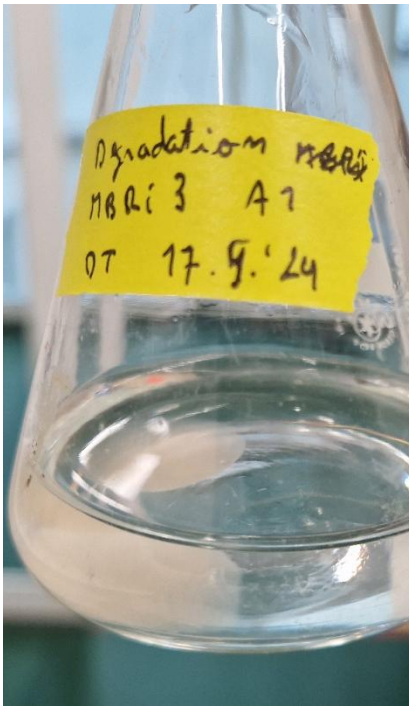

Nin gel in SW #1

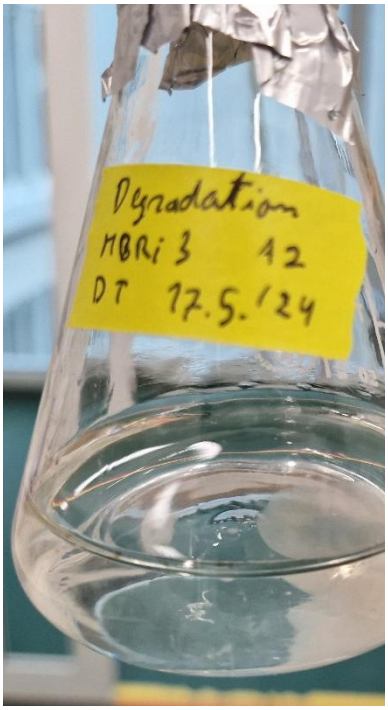

Nin gel in SW #2

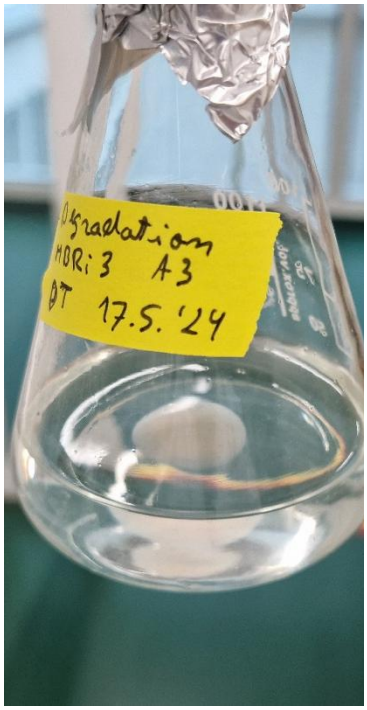

Nin gel in SW #3

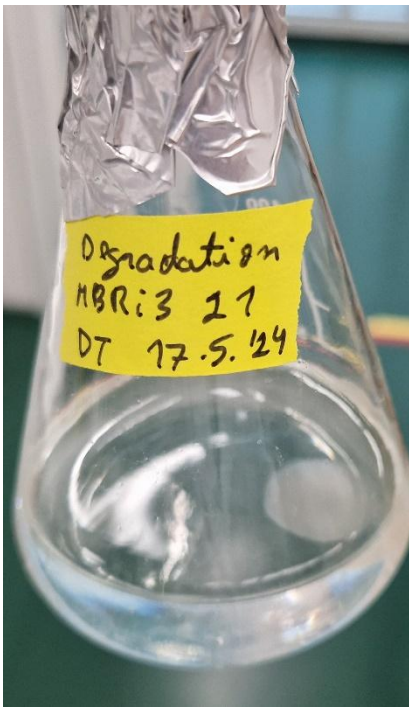

MBRi3 gel in SW #1

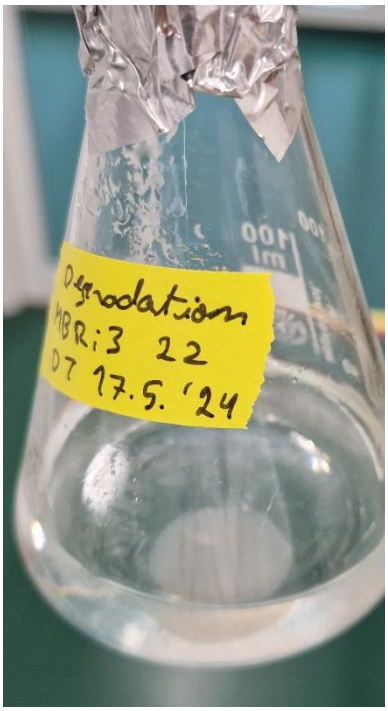

MBRi3 gel in SW #2

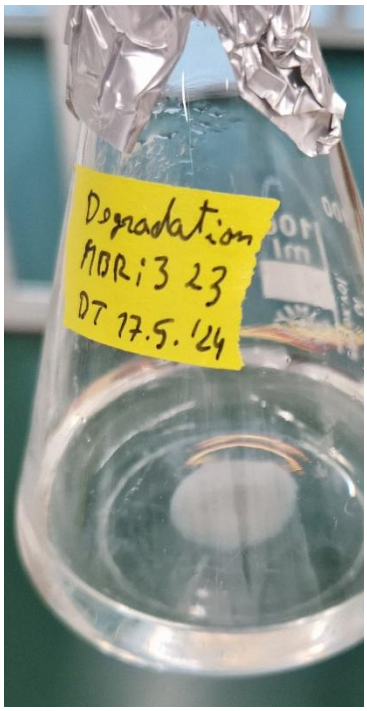

MBRi3 gel in SW #3

- Day 3

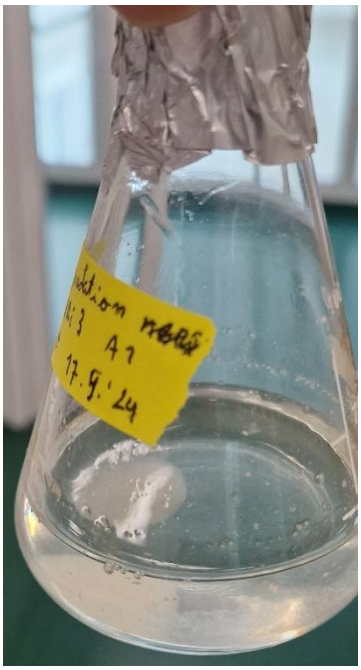

Nin gel in SW #1

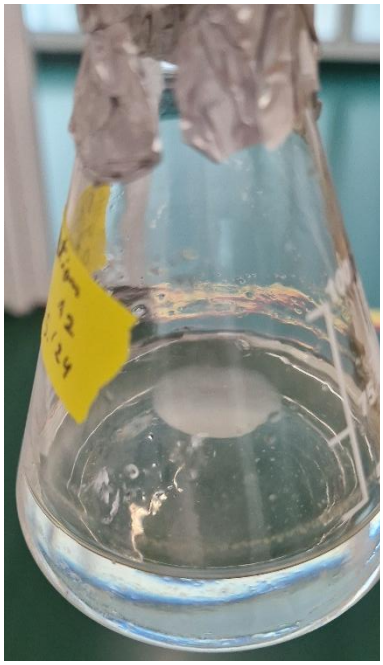

Nin gel in SW #2

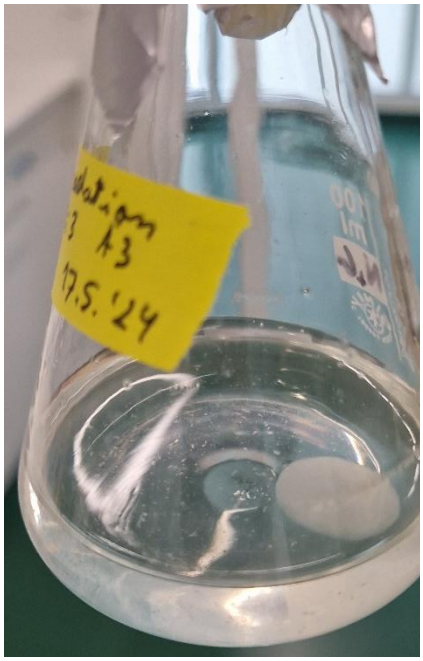

Nin gel in SW #3

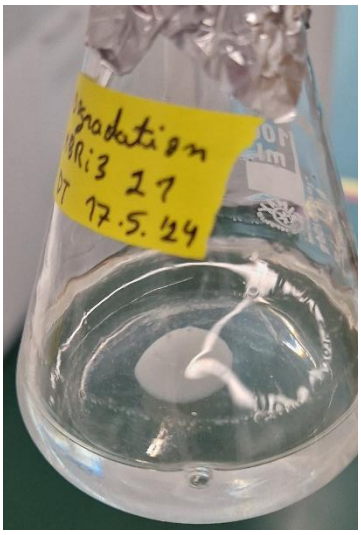

MBRi3 gel in SW #1

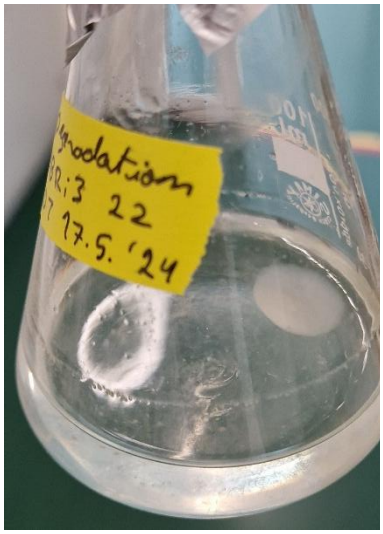

MBRi3 gel in SW #2

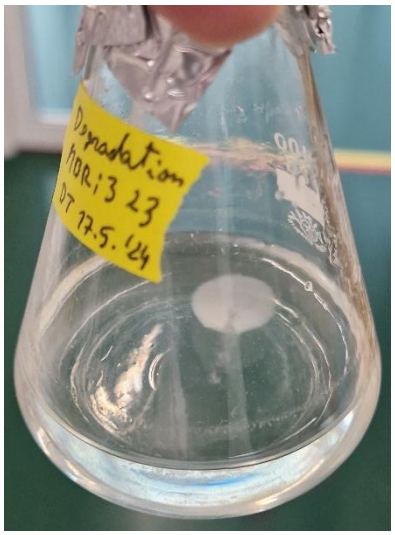

MBRi3 gel in SW #3

- Day 5

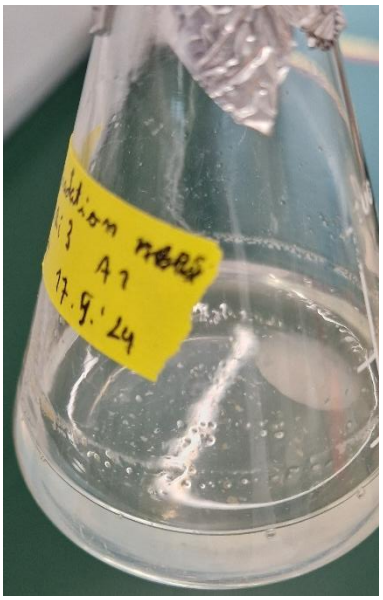

Nin gel in SW #1

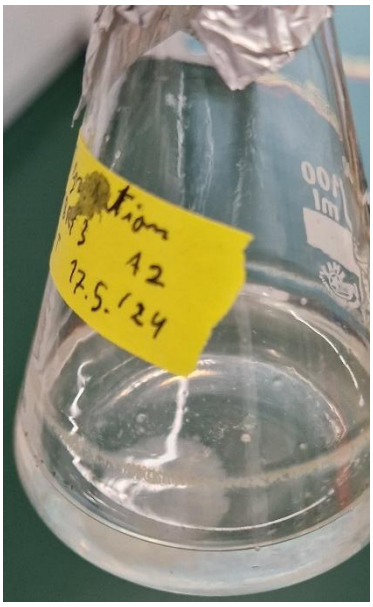

Nin gel in SW #2

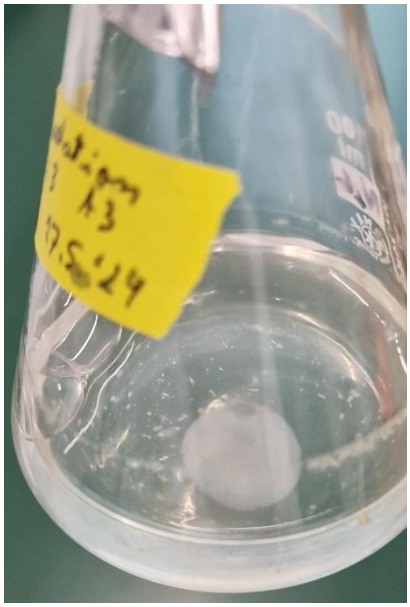

Nin gel in SW #3

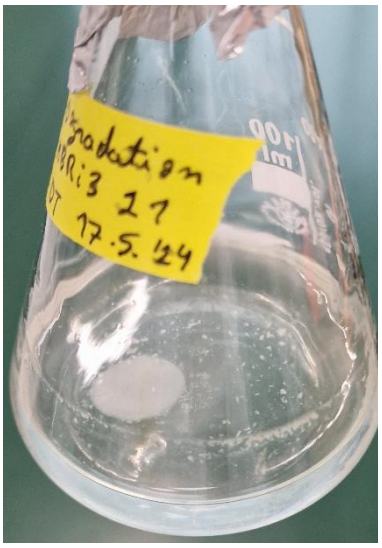

MBRi3 gel in SW #1

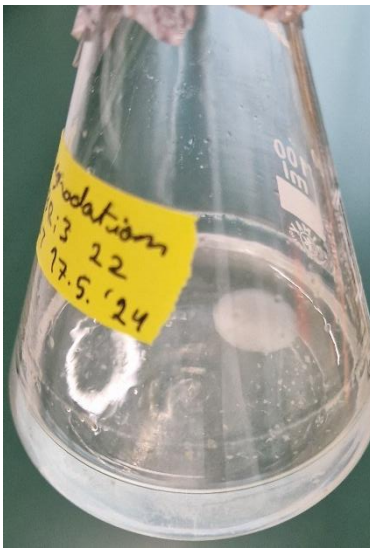

MBRi3 gel in SW #2

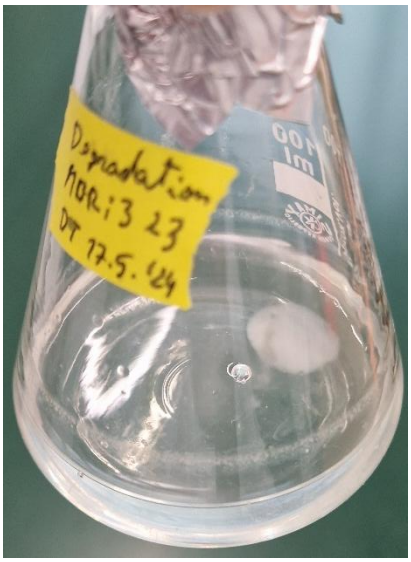

MBRi3 gel in SW #3

- Day 7

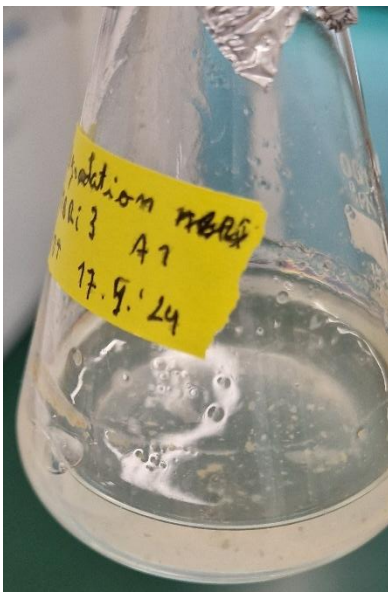

Nin gel in SW #1

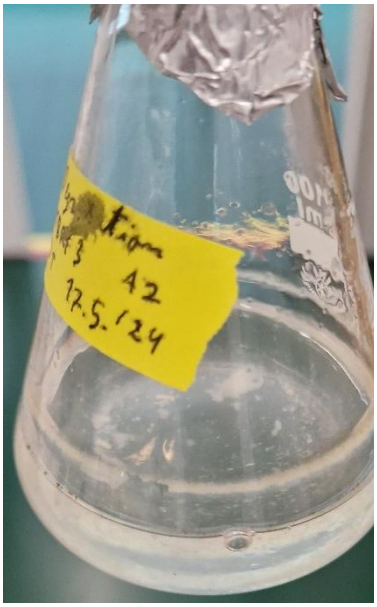

Nin gel in SW #2

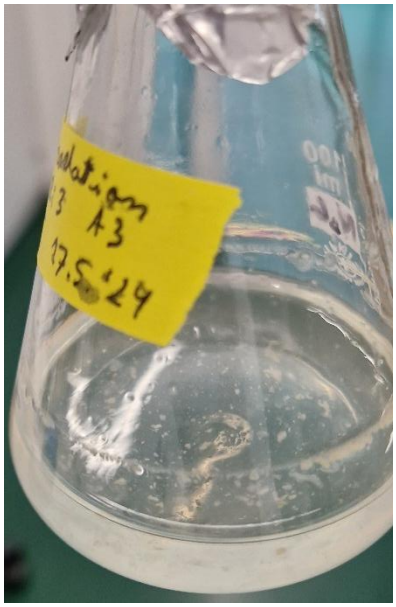

Nin gel in SW #3

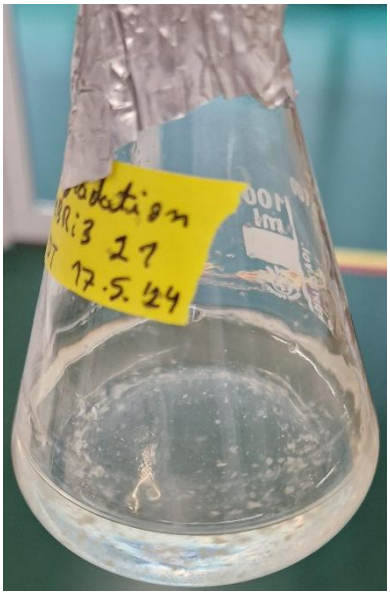

MBRi3 gel in SW #1

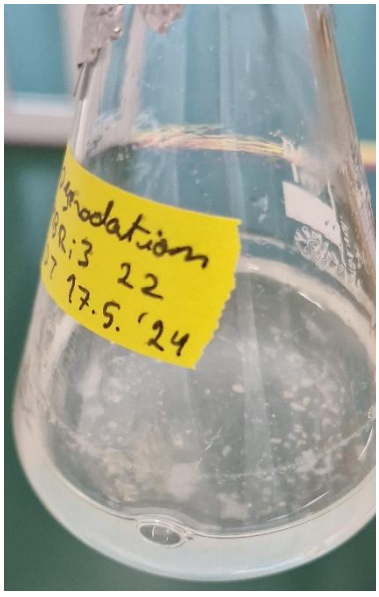

MBRi3 gel in SW #2

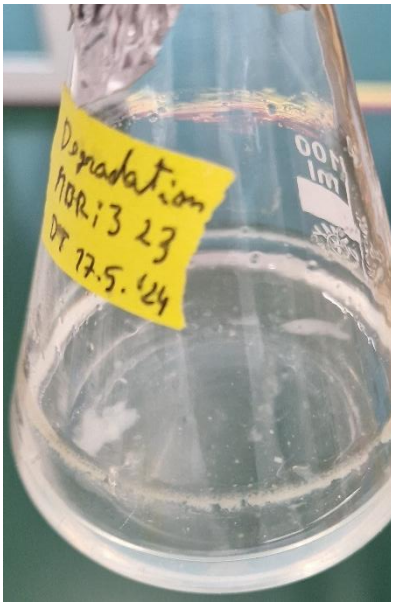

MBRi3 gel in SW #3

7.3 Mann-Whitney U test

7.3.1 Degradation experiment

Table 8 | Mann-Whitney U test's P-values for MBR2 and MBR5 degradation experiment (Figure 5)

P-value	MBR2 bulk in BMM	MBR5 bulk in synGW	MBR5 gel in synGW	MBR5 bulk in BMM
Nin gel in synGW	0.00172	0.27744	0.00601	0.00172
MBR2 bulk in BMM	-	0.02519	0.04667	0.84633
MBR5 bulk in synGW	-	-	0.27744	0.03481
MBR5 gel in synGW	-	-	-	0.04667

Table 9 | Mann-Whitney U test's P-values for MBR2 degradation experiment (Figure 6)

P-value	MBR2 bulk in SW	MBR2 gel in SW	MBR2 bulk in BMM
Nin gel in SW	0.73983	0.51439	0.24512
MBR2 bulk in SW	-	0.73983	0.44179
MBR2 gel in SW	-	-	0.50659

Table 10 | Mann-Whitney U test's P-values for MBRi3 degradation experiment (Figure 17)

P-value	MBRi3 bulk in SW	MBRi3 gel in SW	MBRi3 bulk in BMM
Nin gel in SW	0.44195	0.55411	0.16635
MBRi3 bulk in SW	-	0.74086	0.85011
MBRi3 gel in SW	-	-	0.50833

Table 11 | Mann-Whitney U test's P-values for MBR2 and MB5's cell (Figure 7)

P-value	MBR5
MBR2	0.56444

7.3.2 Survival test

Table 12 | Mann-Whitney U test's P-values for MBR5 survival test, week 1, (Figure 8)

P-value	MBR5 bulk in synGW	MBR5 gel in synGW
Nin gel in synGW	0.75402	0.60151
MBR5 bulk in synGW	-	0.91681

Table 13 | Mann-Whitney U test's P-values for MBR5 survival test, week 2, (Figure 9)

P-value	MBR5 bulk in synGW	MBR5 gel in synGW
Nin gel in synGW	0.14246	0.83404
MBR5 bulk in synGW	-	0.4647

7.3.3 Ink toxicity test

Table 14 | Mann-Whitney U test's P-values for MBR2 and MBR5's cell growth from the ink toxicity test (Figure 10)

P-value		MBR2					MBR5					
		BMM	MA-SA	ι-CA	CMC	CL	Abiotic control	BMM	MA-SA	ι-CA	CMC	CL
MBR2	Abiotic control	0.01796	0.01796	0.00172	0.01796	0.01796	0.44228	0.01796	0.01796	0.00172	0.01796	0.01796
	BMM	-	0.01809	0.03501	0.4822	0.60889	0.01809	0.01809	0.01809	0.84801	0.01809	0.40623
	MA-SA	-	-	0.02535	0.02535	0.01809	0.01809	0.01809	0.11022	0.02535	0.01809	0.01809
	I-CA	-	-	-	0.01809	0.02535	0.00175	0.01809	0.02535	0.14172	0.01809	0.03501
	CMC	-	-	-	-	0.94906	0.01809	0.01809	0.02535	0.74939	0.01809	0.94906
	CL	-	-	-	-	-	0.01809	0.02535	0.01809	0.94906	0.01809	0.5653
MBR5	Abiotic control	-	-	-	-	-	-	0.01809	0.01809	0.00175	0.01809	0.01809
	BMM	-	-	-	-	-	-	-	0.01809	0.01809	0.30615	0.02535
	MA-SA	-	-	-	-	-	-	-	-	0.02535	0.01809	0.01809
	I-CA	-	-	-	-	-	-	-	-	-	0.01809	0.65472
	CMC	-	-	-	-	-	-	-	-	-	-	0.02535

7.3.4 Isolation

Table 15 | Mann-Whitney U test's P-values for MBR2 isolates' IBU degradation (Figure 12)

P-value	1	2	3	4	5	6	7
2	0.26233	0.00789	0.26233	0.07817	0.63095	0.20018	0.05466
3	-	0.0201	0.74877	0.63095	0.52184	0.74877	0.63095
4	-	-	0.03263	0.0201	0.00789	0.03263	0.0201
5	-	-	-	0.87278	0.63095	0.80985	0.74877
6	-	-	-	-	0.33667	1	0.33667
7	-	-	-	-	-	0.52184	0.20018
9	-	-	-	-	-	-	0.52184

Table 16 | Mann-Whitney U test's P-values for MBR2 isolates' cell growth (Figure 13)

P-value	1	2	3	4	5	6	7
2	0.00076	0.00076	0.00855	0.00159	0.01153	0.00075	0.0085
3	-	0.0086	0.01172	0.01166	0.0086	0.00855	0.0086
4	-	-	0.17185	0.00855	0.0016	0.01153	0.00855
5	-	-	-	0.01166	0.0086	0.0116	0.01166
6	-	-	-	-	0.00855	0.0085	0.00855
7	-	-	-	-	-	0.00159	0.08244
9	-	-	-	-	-	-	0.00621

Table 17 | Mann-Whitney U test's P-values for MBR2 diluted cultures' IBU degradation (Figure 14)

P-value	10^{-4}	10^{-5}	10^{-6}
10^{-3}	1	0.00496	0.24613
10^{-4}	-	0.00496	0.24613
10^{-5}	-	-	0.00873

Table 18 | Mann-Whitney U test's P-values for MBR2 diluted cultures' cell growth (Figure 15)

P-value	10^{-4}	10^{-5}	10^{-6}
10^{-3}	0.01166	0.0086	0.03108
10^{-4}	-	0.00992	0.63425
10^{-5}	-	-	0.00992